GENERAL ELECTRIC

GENERAL ELECTRIC COMPANY
CORPORATE RESEARCH AND DEVELOPMENT
Schenectady, N.Y.

INVESTIGATIONS OF LUNAR MATERIALS

FINAL REPORT

January 25, 1972

G.M. Comstock, A.O. Evwaraye, R.L. Fleischer, and H.R. Hart, Jr.

Principal Investigator: R.L. Fleischer

Prepared under Contract No. NAS 9-11583

by

General Physics Laboratory
Corporate Research and Development
GENERAL ELECTRIC COMPANY
Schenectady, New York

for

NATIONAL AERONAUTICS AND SPACE ADMINISTRATION
Manned Spacecraft Center
Lunar Receiving Laboratory
Houston, Texas

GENERAL ELECTRIC

GENERAL ELECTRIC COMPANY, RESEARCH AND DEVELOPMENT CENTER, P.O. BOX 8
SCHENECTADY, NEW YORK 12301, Phone (518) 346-8771

CORPORATE
RESEARCH AND
DEVELOPMENT

INVESTIGATIONS OF LUNAR MATERIALS

FINAL REPORT

January 25, 1972

G.M. Comstock, A.O. Evwaraye, R.L. Fleischer, and H.R. Hart, Jr.

Principal Investigator: R.L. Fleischer

Prepared under Contract No. NAS 9-11583

by

General Physics Laboratory
Corporate Research and Development
GENERAL ELECTRIC COMPANY
Schenectady, New York

for

NATIONAL AERONAUTICS AND SPACE ADMINISTRATION
Manned Spacecraft Center
Lunar Receiving Laboratory
Houston, Texas

INVESTIGATIONS OF LUNAR MATERIALS

by

G.M. Comstock, A.O. Evwaraye, R.L. Fleischer, and H.R. Hart, Jr.

General Physics Laboratory
Corporate Research and Development
General Electric Company
Schenectady, New York

ABSTRACT

This report presents the work done and reported under contract NAS 9-11583. The investigations were directed at determining the radiation history and surface chronology of lunar materials using the etched particle track technique. As reported in detailed papers included as appendices, the major lunar materials studied or reported on in this period are the igneous rocks and double core from Apollo 12, the breccia and soil samples from Apollo 14, and the core samples from Luna 16. In the course of this work two new and potentially important observations were made: i) Cosmic ray induced spallation-recoil tracks were identified. The density of such tracks, when compared with the density of tracks induced by a known flux of accelerator protons, yields the time of exposure of a sample within the top meter or two of the moon's surface. ii) Natural, fine scale plastic deformation was found to have fragmented pre-existing charged particle tracks, allowing the dating of the mechanical event causing the deformation. The most recent work is reported in Appendices I through III, the extended abstracts submitted at the Third Lunar Science Conference, January 1972.

TABLE OF CONTENTS

INVESTIGATIONS OF LUNAR MATERIALS

by

G.M. Comstock, A.O. Evwaraye, R.L. Fleischer, and H.R. Hart, Jr.

SUMMARY AND GUIDE TO APPENDED PAPERS

The experimental accomplishments and scientific reporting of this contract period are given in detail in Appendices I through VIII of this report. Appendices I through III are the extended abstracts or short papers submitted at the Third Lunar Science Conference, January 10-13, 1972, and describe our most recent work. The remaining appendices are scientific papers which have been published or submitted for publication.

The igneous rocks returned by the Apollo 12 mission yield iron group cosmic track densities (see Appendix IV) which imply surface residence times that range from $< 10{,}000$ years to ~ 24 million years. The steep track gradients at exposed surfaces show that some rocks have been on the lunar surface in one position only; others have been turned over at least once. Spallation recoil track densities were used for the first time to determine the times of exposure of rocks in the top meter or two of the moon's surface. These spallation track exposure times range from ~ 20 to 750 million years. Fine scale erosion rates of lunar rocks were estimated by comparing

the near surface cosmic ray track distributions with that found in an uneroded glass detector exposed in Surveyor III. An erosion rate for igneous rock surfaces of about one atomic layer per year was obtained.

The Apollo 12 double core sample yields (see Appendix V) cosmic ray and spallation recoil track density distributions which indicate stirring of the soil in layers as deep as 60 cm.

The double core results are analyzed in much greater detail in a comprehensive review paper (Appendix VI) covering the history of the lunar surface as revealed by fossil particle tracks. In this discussion a model for soil excavation, layering, and burial is presented and compared with the core results. In addition, the relation between iron group cosmic ray track densities and surface residence times is carefully scrutinized.

Electron microscope examination of replicas of etched lunar crystals has allowed the identification of a new phenomenon, the deformation-induced erasure of particle tracks (Appendix VII and, more recently, Appendix II). The fossil damage trail left by a charged particle is seen to be severed into several shorter fragments by fine scale, plastic deformation. An observer using an optical microscope would see only the tracks formed after the deformation, and would thus date the

event causing the deformation. With this recognition, one can date soil and breccia forming events.

Particle track counts taken on Luna 16 samples (Appendix VIII and, more recently, Appendix III) reveal an extremely heavy irradiation with only minor differences from the top to the b ottom of the core. Assuming no net influx of surface irradiated material at the Luna 16 site we surmise that the regolith is here not much thicker than the 30 cm sampled.

The wide track density distributions found in the breccias from the Apollo 14 mission (Appendix I) indicate that the tracks in some grains are retained through the brecciation event while others are totally or partially erased. By assuming that the lowest track densities observed correspond to grains undergoing complete track erasure in the breccia formation, we can place upper limits on the surface residence times of these rocks. The times found are shorter than those of the igneous rocks of Apollo's 11 and 12, indicating perhaps that the friable nature of the breccia leads to a more rapid loss of surface material or to a greater likelihood of total disintegration upon a meteroid impact. The Apollo 14 soil samples yield a wide range of track densities, varying from a young soil at Cone Crater to a much older soil at the landing site.

APPENDIX I

Third Lunar Science Conference

THE PARTICLE TRACK RECORD OF FRA MAURO, H.R. Hart, Jr., G.M. Comstock, and R.L. Fleischer, General Electric Research and Development Center, Schenectady, New York 12301.

Apollo 14 breccias, igneous rocks, and soils and two Apollo 15 soils have been analyzed by means of cosmic ray tracks. The most abundant Apollo 14 rocks, the breccias, have a mixture of high and low track densities at most positions in their interior. The observed track abundances make it clear that most of the tracks are inherited from the parent ingredients of the breccias. Measurement of the minimum track density at a known depth allows a maximum surface exposure time at that depth to be calculated. Since shock - the probable agent for producing these breccias - does erase tracks in some of the crystals, it is likely that in most cases the minimum densities are in fact true values for the number of tracks created since formation of the breccias. The observed maximum surface residence times (see Table I), 0.05 to 8.2 m.y. with a median of 1.35 m.y., are typically a factor of ten less than those observed for Apollo 11 and 12 igneous rocks. The low surface exposures appear to be the natural result of the friable nature of these rocks, which allows more rapid large scale erosion and more catastrophic break-up from impacts.

The only igneous Apollo 14 rock of interest is 14310. Our data on a section extending from the center of the rock to the bottom would be compatible with 1 m.y. surface exposure of the bottom followed by a 20 m.y. exposure in the upright position. Data from other members of the 14310 consortium, however, make it clear that a more complicated history must have obtained. One possibility is that the major surface exposure occurred over a longer time with the present rock 14310 as the interior of a considerably larger rock (at least 20 cm in radius, for at least 400 m.y.). Three igneous rocks in the size range 2-4 mm give surface ages of 3, 3, and 5 m.y.

Examination of gradients in a group of soil samples reveals variable slopes, most of which are artificially low because the samples were cut at random - i.e., without knowledge of the direction of the original nearest, space-exposed surface. The steepest slope is consistent with the spectrum inferred from the Surveyor III filter glass, and yields a surface residence time of 4500 years ($\pm$35%).

Soils are extremely variable - median track densities ranging over at least a factor of 200. Soil from the bottom of the trench at site G (Apollo 14) has track densities typically a factor of 20 to 60 less that of nearby surface soils 14259 and 14163. The youngest soil we have examined is 15401, which is rich in clear, defect-free green glass spherules and ellipsoids.

Median track densities in the green glass and pyroxenes suggest that most of this soil is unusually young. Assuming it was scooped from depths ranging from 0 to 3 cm, we infer a deposition not more than 10^6 years ago.

SURFACE AGES OF BRECCIAS

ROCK NUMBER	MIN. TRACK DENSITY [$\times 10^6/cm^2$]	MAXIMUM DEPTH [cm]	MAXIMUM SURFACE AGE [$\times 10^6$ YR]
14047, 42	1.1	0.5	3.4
14055, 1	0.07	0.6	0.05
14066, 22	0.47	0.7	0.49
14301, 33	0.27	0.5	0.34
14311, 36	0.73	3.5	3.1
		0.5	1.1
14321, 270	0.39	10.8	8.2
15233, 5, 3	14	0.15	7.4
15233, 5, 14	1.6	0.08	0.3
15233, 5, 16	7.0	0.09	1.4
15233, 5, 17	3.5	0.13	1.3
		MEDIAN	1.35
		MEDIAN FOR APOLLO 11 AND 12	13

APPENDIX II

Third Lunar Science Conference

PARTICLE TRACK DATING OF MECHANICAL EVENTS, R.L. Fleischer, H.R. Hart, Jr., and G.M. Comstock, General Electric Research and Development Center, Schenectady, New York 12301.

"Dating" of mechanical events by deformation-induced erasure of particle tracks is made possible by virtue of the fact that natural, fine scale plastic deformation can fragment pre-existing charged particle tracks in lunar crystals, as sketched in Figure 1. Many examples of such effects have been identified in electron micrographs of etched lunar soil grains. In one case, sample 12028, 111, 30.3, 2, slip lines cover the field of view and are correlated with the track lengths: Where the slip spacing is relatively wide ($\gtrsim$0.7 microns) the tracks are typically $\sim$0.7 microns long; where the slip spacing is reduced to $\sim$0.07 microns, the track length is correspondingly less. In the light microscope (Leitz Ortholux at 1350X magnification) no tracks are visible in the region of fine slip, and recognizably short tracks are just discernible in the region of coarser slip. Superimposed on the approximately $3 \times 10^8/cm^2$ short tracks are $\sim 3 \times 10^5$ longer tracks that are uniformly distributed with no differences between the regions of fine and coarse slip. These longer tracks presumably correspond to irradiation of the sample by cosmic rays subsequent to the event which fragmented the

original tracks and hence should allow the deformation history to be inferred.

Since deformation markings are abundant features in lunar soil, their effects provide a powerful tool for constructing deposition histories for stratified soil samples. When many crystals are examined in a given soil layer, it is likely that several of these have been "reset" by the impact that laid down that layer. If we assume that the lowest track density observed in a layer came from near the bottom of that layer, we can compute a surface exposure time. For the long Apollo 12 core (12025 + 12028), we compute intervals ranging from 2 to 60 million years for various sublayers, with an accumulated time of 220 million years for samples for which Arrhenius et al[1] inferred a 310 million year surface exposure. The difference may be attributed to Arrhenius et al's using the lower quartile of their track density distribution instead of the lowest track density observed. Their assumption of no predepositional surface residence for these samples yields a higher age. A similar analysis, assuming that Apollo 11 core 10005 is composed of three layers, gives an integrated surface age of 40 to 75 million years for its 10.5 cm depth.

1. G. Arrhenius, S. Liang, D. Macdougall, L. Wilkening, N. Bhandari, S. Bhat, D. Lal, G. Rajagophalan, A.S. Tamhane, and V.S. Venkatavaradan, Geochim. Cosmochim. Acta Suppl. 2, 3, 2583 (1971).

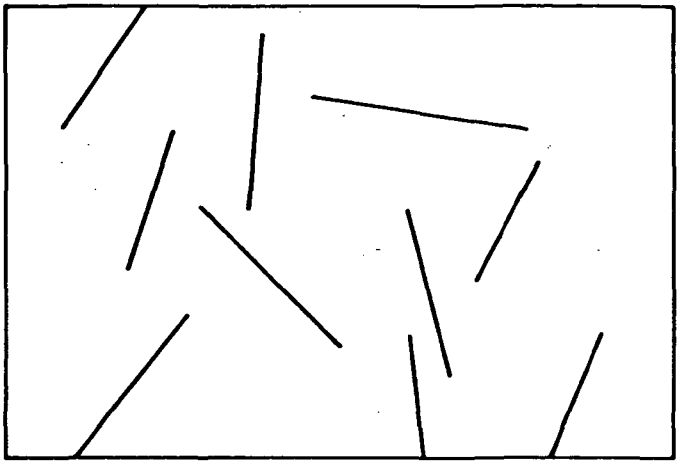

CRYSTAL WITH TRACKS

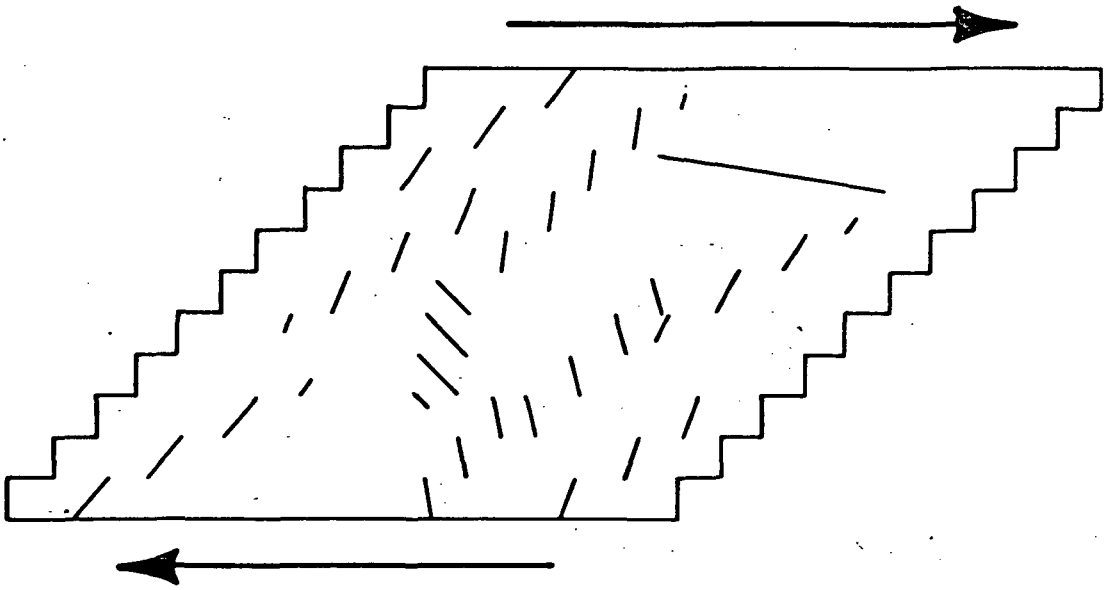

CRYSTAL WITH TRACKS AFTER DEFORMATION

APPENDIX III

Third Lunar Science Conference

PARTICLE TRACK RECORD OF THE SEA OF PLENTY, G.M. Comstock, R.L. Fleischer, and H.R. Hart, Jr., General Electric Research and Development Center, Schenectady, New York 12301.

Particle track counts in 41 crystals taken from layers 1 and 4 of the Luna 16 core sample reveal only slight differences between the two levels. The high track densities we observe indicate that virtually all of the grains have been highly irradiated, on or near the surface for a great length of time (in contrast to Apollo 11 and 12 soils which include many grains with $<10^8$ tracks/cm^2). Grains could have acquired the observed median density of 1-2 x 10^9/cm^2 in $\sim 10^6$ years on the very surface (for $\sim$100-μ diameter grains) or in $\sim 3 \times 10^9$ years at a depth of 1 cm. Since there are 3000 100-μ layers in 30 cm (the depth to level 4), the total time required for each of them to have spent $\sim 10^6$ years on the surface is also $\sim 3 \times 10^9$ years, comparable to the age of the maria surfaces. Not only have nearly all of the Luna 16 grains been very close to the surface, but there has also been little "recent" admixture of previously shielded and therefore low track density material from below 30 cm. Further there is no time available in the "exposure budget" for material much below 30 cm at the Luna 16 site to have been exposed near the surface. We conclude that the regolith is unusually thin at

the Luna 16 site. This is consistent with the observation that the Luna 16 core coarsens near the bottom.

The slight decrease in median track density observed in going from layer 1 to layer 4 is consistent with the results of Kashkarov on olivines from layers 1 through 5. Our cumulative track density distribution is given in Table I and the detailed distributions in Figure 1.

Table I: Cumulative Track Density Distribution

DENSITY[cm^{-2}]	LEVEL 1	LEVEL 4
$>4 \times 10^7$	100%(20)	95%(20)
$>10^8$	100%(20)	90%(19)
$>10^9$	>35%(7)	>33%(7)

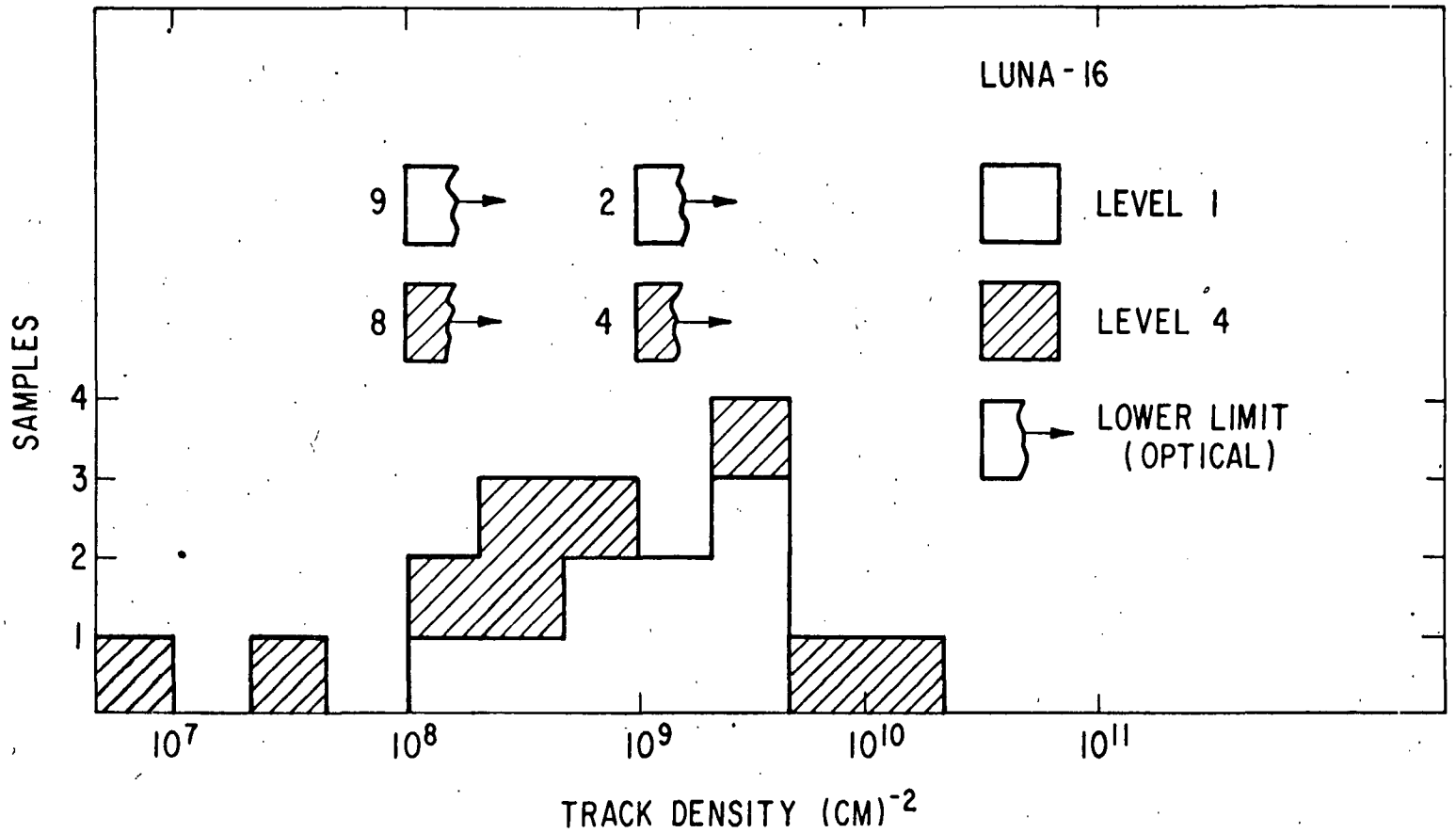

Distribution of track densities from Level 1 (0-8 cm) and Level 4 (28-32 cm). All definite values were measured using a transmission electron microscope. In addition, the numbers to the left of the broken bars with arrows indicate the numbers of crystals for which lower limits have been estimated optically.

APPENDIX IV

Geochim. Cosmochim. Acta, Supplement 2

GENERAL ELECTRIC

REPRINT 6907

GENERAL ELECTRIC COMPANY
CORPORATE RESEARCH AND DEVELOPMENT
P.O. Box 43, Schenectady, N.Y. 12301 U.S.A.

THE PARTICLE TRACK RECORD OF THE OCEAN OF STORMS

R.L. Fleischer, H.R. Hart, Jr.,
G.M. Comstock and A.O. Evwaraye

Proceedings of the Second Lunar Science Conference, Vol. 3, pp. 2559–2568
The M.I.T. Press, 1971.

The particle track record of the Ocean of Storms

R. L. FLEISCHER, H. R. HART, JR., G. M. COMSTOCK, and A. O. EVWARAYE*
General Electric Research and Development Center, Schenectady, New York 12301

(*Received* 22 *February* 1971; *accepted in revised form* 29 *March* 1971)

Abstract—In Apollo 12 rocks the numbers of tracks from the solar and galactic iron group cosmic rays imply surface residence times that range from $< 10{,}000$ years to ~ 30 million years. The presence of steep track gradients at exposed surfaces shows that some rocks have been on the lunar surface in only one position, while others have been turned over and moved more than once. For example, rock 12017 was raised to within one meter of the surface, later thrown to the very surface, then flipped over and recently splattered with molten glass (just 9000 years ago). The abundance of nuclear interaction (spallation) tracks induced by the penetrating galactic protons provides residence times for different rocks in the top meter of soil of ~ 20 to 750 millions of years. The erosion of lunar rocks is estimated by comparing the cosmic ray track distributions in lunar rocks with the one found in an uneroded glass detector exposed in Surveyor III. Erosion at a rate of about one atomic layer per year is inferred. By inducing uranium-235 fission tracks we have measured widely ranging uranium concentrations: less than 10^{-3} parts per million in pyroxenes, ~ 1 ppm in glass, and up to 170 ppm in zircon. The fossil track abundance in the zircon gives no evidence for the presence of extinct radioactivity by plutonium-244 or by super-heavy nuclei.

INTRODUCTION

THE ABUNDANT particle tracks found in most lunar samples constitute a highly detailed record of the diverse chronology of lunar samples. Solidication ages are recorded by uranium-238 fission tracks (PRICE and WALKER, 1963a; FLEISCHER and PRICE, 1964a, b); times of exposure on the lunar surface (*surface residence* times) are given by tracks or iron group nuclei in the cosmic rays (CROZAZ *et al.*, 1970a; FLEISCHER *et al.*, 1970a, later PRICE and O'SULLIVAN, 1970; LAL *et al.*, 1970) and we shall see that nuclear interaction (spallation) tracks (FLEISCHER *et al.*, 1970a, b) measure the total time spent near and at the lunar surface.

PROCEDURES

The primary new technique employed in this work is the use of spallation tracks to measure the total time near the lunar surface. We have found that spallation tracks yield ages that agree with radiometrically measured cosmic ray exposure times. For other procedures, including etchants used, our previous work (FLEISCHER *et al.*, 1970b) should be consulted.

Technique for measuring spallation ages

Previously (FLEISCHER *et al.*, 1970b) we demonstrated that the short, nearly featureless tracks (FLEISCHER *et al.*, 1967) produced by nuclear interactions of penetrating primary cosmic ray particles increase in number with the time of exposure in the top 1–2 meters of soil. At the same time we noted that the observed density of these tracks varied appreciably from grain to grain, even though there is little variation with position in rocks of the sizes that have been available from Apollo 11 and Apollo

* Present address: Department of Physics, Antioch College, Yellow Springs, Ohio.

12. The observed grain-to-grain variation in rocks is most likely a variation of etching efficiency that depends primarily (as judged by etching different portions of a fragmented crystal) on the crystallographic orientation of the etched surface and very likely on compositional variations, but only secondarily on the etching time, and very little (FLEISCHER *et al.*, 1967) on the orientation relative to the incident cosmic ray nuclei. A reproducible measurement is made by etching a number of grains of the minerals of interest (in this case, pyroxenes) and choosing the highest track densities present as representative of the highest etching efficiency.

As long as this procedure is used in obtaining both the natural track counts (ρ_{sp}) and the calibration counts (P) that measure production rates, the ratio ρ_{sp}/P will be reproducible on a given rock. Ideally the irradiation and the subsequent calibration would be done for the same crystals as the natural track counts.

The production rate P is measured for individual surface samples by bombarding annealed (track free after 17 hours at 820°C in platinum boats) samples with 3 GeV protons from the Princeton-Pennsylvania Accelerator in order to simulate the nuclear-active cosmic rays incident upon the moon. In reality these active particles include not only protons but primary helium and heavier nuclei and secondary high energy neutrons and pions. At the very surface the protons and alphas dominate. Although minor errors are introduced in calibrating with a single type of particle at a single energy, they are small relative to the variations inherent in the uncertainties of individual rock histories as to depths of burial and detailed geometries and compositions of shielding material. As judged by the etching of annealed samples following irradiation with fission fragments, the thermal treatment has not altered the registration properties of the pyroxenes.

RESULTS

Spallation ages and proton doses

In the preceding section we indicated how reproducible values are measured for the ratio of the spallation track density ρ_{sp} to the production rate P of recoil tracks caused by high energy protons. The ratio ρ_{sp}/P is the dose of protons needed to produce the observed spallation track density. In Table 1 measured values of ρ_{sp}/P are given for a group of lunar samples in the column headed Proton Exposure. By assuming a flux ϕ of $3 \times 10^7/\text{cm}^2\text{-yr}$ of primary cosmic ray nucleons (BAZILEVSKAYA *et al.*, 1968) we calculate spallation Surface Ages given in the next column of Table 1 by $\rho_{sp}/P\phi$, the spallation ages if the entire proton exposure occurred on the lunar surface.

For samples such as those listed, which were all picked up at the surface, these ages should be to first approximation directly comparable with the radiometrically measured spallation ages—listed in the right-hand column of Table 1. In general the agreement is excellent, well within the scatter among different radiometric ages where more than one such age is available. In a higher approximation the agreement between the radiometric age and the track spallation surface age depends on the detailed burial history of the rock. Different track and radiometric ages for samples with complex burial histories will result if the cross-sections for the individual relevant spallation reactions vary differently with depth of burial (HONDA and ARNOLD, 1964). In addition, differences can arise if a sample is exposed at depth and then moved to the surface at a time that is recent with respect to the half life of the nuclide being used to measure the production rate radiometrically.

The true proton exposure ages are uncertain, however, because we do not know the samples' depths of burial during proton exposure. As accelerator experiments have shown (HONDA and ARNOLD, 1964), a cascade of nuclear-active, secondary

Table 1. Track spallation ages of lunar pyroxenes.

Sample Number	Production rate (P)* (tracks/10^9 protons)	Observed track density (ρ_{sp}) (cm^{-2})	Proton exposure (ρ_{sp}/P) (protons/cm^2)	Surface age (10^6 yr)	Minimum spallation age (10^6 yr)	Radiometric spallation ages (10^6 yr)
10017	1.7†	$2.1(\pm0.1) \times 10^7$	1.2×10^{16}	420	170	200–640[a,e,f,g,i,j]
10044	1.0	$8.2(\pm1.2) \times 10^6$	8.2×10^{15}	270	110	56–100[f]
10049	2.39	$1.49(\pm0.15) \times 10^6$	6.2×10^{14}	21	8.5	22.5–25[g,i]
12002	1.7†	$2.66(\pm0.25) \times 10^6$	1.6×10^{15}	55	20	50–145[b,d,h]
12017	1.45	$4.57(\pm0.32) \times 10^6$	3.2×10^{15}	105	40	—
12021	2.31	$5.1(\pm0.3) \times 10^7$	2.2×10^{16}	740	300	300[h]
12065	1.35	$6.81(\pm0.28) \times 10^6$	5.1×10^{15}	170	70	160–200[c,k]

* Absolute values uncertain to ±30%, but relative values are valid for 10049, 12002, 12017, 12021, and 12065.

† Average of other values.

[a] ALBEE *et al.* (1970); [b] ALEXANDER *et al.* (1971); [c] BLOCH *et al.* (1971); [d] D'AMICO *et al.* (1971); [e] EBERHARDT *et al.* (1970); [f] FIREMAN *et al.* (1970); [g] HINTENBERGER *et al.* (1970); [h] MARTI and LUGMAIR (1971); [i] MARTI *et al.* (1970); [j] O'KELLEY *et al.* (1970); [k] STOENNER *et al.* (1971); [l] From measurements by FUNKHOUSER *et al.* (1970).

protons and neutrons builds up with depth and then attenuates. From the data of FLEISCHER *et al.* (1967) we estimate that in order to produce optically visible, etched tracks from spallation recoil nuclei, reactions are required in which at least 5 nucleons are ejected from the struck nucleus. In such reactions the maximum flux is ~2.5 times the primary proton flux and occurs at a depth of about 20 to 25 cm of soil (or 10 to 12 cm of rock) (KOHMAN and BENDER, 1967). The column labeled Minimum Spallation Age in Table 1 gives minimum times corresponding to burial at a 25 cm soil-equivalent depth. It should also be evident that the observed track densities could have been produced by much longer exposures than we have listed, if the samples were located at greater depths where the high-energy particle flux is corresponding lower.

At present, track spallation ages are of relatively low precision. They do, however, give reasonable agreement with the radiometric ages, and they give track workers a new tool for assessing radiation exposure histories. So far, we report spallation results only for pyroxenes. However, by measuring spallation ages for another mineral with an identical track registration threshold, an improved internal check on the accuracy of such ages will be possible. By measuring ages using minerals of different thresholds and therefore different depth variations of the track production rate, data on depths of burial will be obtained. As we shall see, comparison of spallation track ages with surface residence ages calculated from the track densities from heavy cosmic rays also yields such data.

Tracks of heavy cosmic rays: rock 12017

We have shown previously (CROZAZ *et al.*, 1970; FLEISCHER *et al.*, 1970a) how the dominant cosmic ray tracks from the iron-group nuclei can be used to measure the surface residence times of rocks and rock fragments, and how from steep track density gradients near space-exposed surfaces, former orientations of rocks can be inferred. As an example, the results shown in Fig. 1 for rock 12017 allow us to derive solely from track data the complicated and varied history given in Table 2.

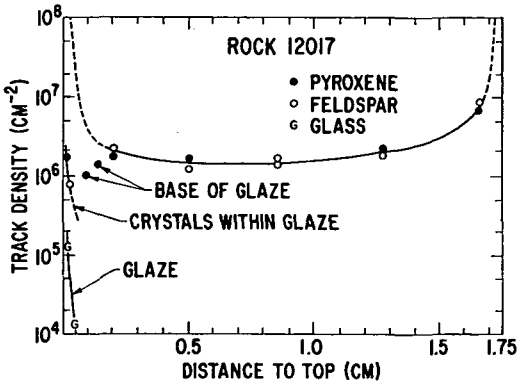

Fig. 1. Cosmic ray track distribution in rock 12017. The top of this rock was coated with glass of maximum thickness 0.15 cm. Tracks in crystals within the glass show it to be recently formed. Pyroxene and glass track densities are corrected for the measured etching efficiencies of 0.7 and 0.08.

Spallation tracks indicate the period over which the rock was exposed to galactic cosmic rays, and they are responsible for the first two entries in Table 2. The increases in cosmic-ray track density near both surfaces show that both sides have been exposed to space, and the slight asymmetry in the profile shows that the bottom received the longer exposure, roughly 1 million years, as compared to 7×10^5 years for the top. At the very top is a glass coating that apparently was splashed on after the rock was positioned with that side up. From (presumably annealed) crystals trapped within the coating its space exposure is inferred to be only $\sim$9000 years, using the track production rate given by FLEISCHER *et al.* (1970b). The glass itself (microprobe analysis by wt.%: SiO_2, 46.4; FeO, 17.7; Al_2O_3, 10.5; MgO, 11.0; CaO, 9.30; TiO_2, 2.80) has the track retention characteristics given in Fig. 2. This glass is not highly retentive, allowing fading in 2 years at 400°K and 500 years at 350°K. We estimate that with the thermal cycling that occurs on the moon, tracks in a glazed rock with estimated peak temperature 360°K, would only be preserved over (very roughly) the last 500 years, as explained further in the caption to Fig. 2. We note parenthetically that in the glass there is a pronounced additional track fading that produces a decrease in track density toward the surface in the top 30 μ, a distance that corresponds to two or three optical depths for visible light. The cause of this effect has not been identified.

Table 2. Simplest track chronology for rock 12017.

Time (years before present)	Event
up to $\sim$ 105,000,000	Buried > 200 cm
$\sim$ 105,000,000	Moved to < 200 cm and >15 cm
$\sim$ 1,700,000	Moved to surface
$\sim$ 700,000	Flipped over
$\sim$ 9000	Splattered with hot glass
$\sim$ 500 to 0	Glass records solar flare particles

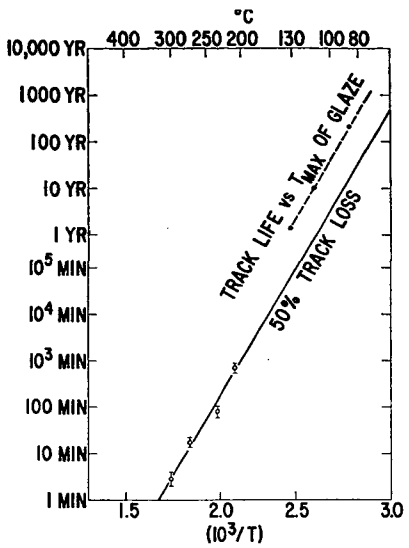

Fig. 2. Track retentivity in the glaze on rock 12017. Extrapolation of the data from lower temperatures predicts 50% track fading after one month continuously at 400°K. The dotted line indicates probable track life on the surface of the moon as a function of the maximum temperature reached by the glaze at lunar noon. Temperature vs. time data from the infra red measurements of SINTON (1962) were used.

In summary the low-energy cosmic rays (dominantly solar flare particles) have been recorded over different time intervals: the glaze over the last 40 to 50 solar cycles, the crystals within the glaze over the last ~ 800, and the bottom of the rock over a more ancient group of $\sim 500{,}000$ cycles. Track distributions in these three sites should allow the proposed (PRICE and O'SULLIVAN, 1970) "solar flare paleontology," comparing ancient solar spectra at different periods of time.

Surface residence times

Table 3 Summarizes cosmic-ray track information for Apollo 12 rocks and gives the most current data on 10049. This is an Apollo 11 rock of special interest because its surface time of 29 m.y. agrees with the 24 m.y. inferred from radioactivity measurements of spallation-produced nuclides (FUNKHOUSER *et al.*, 1970; HINTENBERGER *et al.*, 1970) and the 21 m.y. inferred here from spallation tracks. In short this sample spent all of its near surface time directly exposed to space and underwent very little erosion (which would have lowered the track density). The limit on erosion ($< 3 \times 10^{-8}$ cm/yr) is consistent with what we will infer shortly in this paper from our Surveyor III results. Table 3 shows a wide range of surface exposure times—from $\sim 10^4$ to 3×10^7 years—for samples some of which have been in a single surface position, some in at least two positions, and one in at least three.

The Surveyor III data has also made possible more reliable measurements of short surface residence times of small grains. Here the most abundant tracks are solar

Table 3. Minimum cosmic ray track densities and surface residence times for lunar samples.

Sample	Mineral	Track density (cm^{-2})	Depth in sample (cm)	Surface residence time (million years) (top/bottom)
10049	Pyroxene	1.55×10^7	0.90 cm	(29 total)
12002	Pyroxene	2.8×10^6	5.0	(24/0)
12017	Feldspar	1.51×10^6	0.45	(0.7/1.0)
12017	Feldspar in glaze	8×10^5	0.02	(0.009/0)
12021	Pyroxene	5.0×10^6	4.0	(13/13)*
12065	Pyroxene	2.2×10^6	6.4	(14/0)
12025, 12028 (Soil)	Pyroxene, Feldspar	3×10^7†	—	(110 total)‡
12025, 4, 54–8.5, 9, 9	Pyroxene	5×10^7	0.002	0.01/0)§

* This result disagrees with that of PRICE (personal communication); a mix-up in sample position designation (either his sample or ours) is suspected.
† Average of 100 μ–400 μ diameter grains.
‡ Average time in top 60 cm of soil, calculated in same manner as in FLEISCHER *et al.* (1970b).
§ Using solar spectrum from Surveyor III glass (FLEISCHER *et al.*, 1971) after adjustment for solar cycle.

heavy cosmic rays whose flux previously was highly uncertain. Because of the presence in most lunar samples of an unknown amount of erosion, the track production rate vs depth was only a lower limit. However, with the recent data (adjusted to solar cycle average) for the uneroded Surveyor III glass and the assumption that it represents a typical solar cycle, the ages can be computed for small grains such as that sketched in Fig. 3. The steep track gradients mapped around roughly half of its perimeter reveal that at one time this grain was exposed directly to space, as a small grain resting on what is drawn as its right side. By matching the steepest gradient in this grain with calculations based on the Surveyor III flux of solar heavies (FLEISCHER *et al.*, 1971) a surface residence time of 10,000 years is obtained. This age would be altered somewhat if the solar fluxes are used that have been inferred by CROZAZ and WALKER (1971) or PRICE *et al.* (1971) from the same material. Hence, the absolute surface time for this sample is subject to possible revision, but is roughly correct and clearly much shorter than the 0.5 to 30 m.y. that typifies most larger moon rocks.

Burial and burial depths

By comparing track spallation ages with track surface residence times and with radiometric spallation ages, permissible burial depths can be inferred. Thus for rock 10049, where all three agree, the entire exposure must have been at the surface. For the other rocks listed, where the surface residence age is shorter than the spallation age, the samples must have been buried over most of their spallation exposure times.

Lunar erosion

In a separate experiment (FLEISCHER *et al.*, 1971) using tracks etched in a glass optical filter from the Surveyor III television camera we have measured the energy spectrum of the iron group solar cosmic ray particles over the energy range 1 to 100 Mev/nucleon, finding for the differential flux $1.8 \times 10^3\ E^{-3}$ particles/m^2-sec-str-MeV/nucleon. We have also observed high energy fission of Pb, induced by galactic cosmic ray protons and alpha particles.

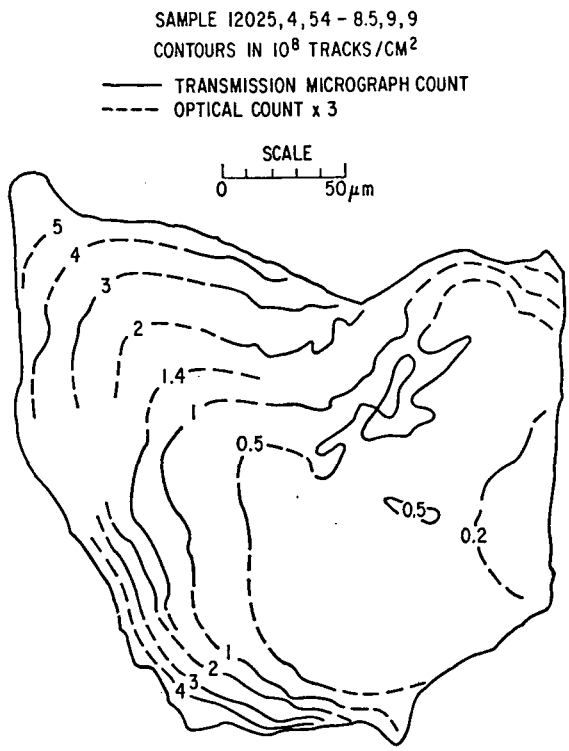

Fig. 3. Cosmic ray track density distribution in a grain found at 8.5 cm depth in core 12025. The gradients identify the surfaces exposed directly to space and to heavy cosmic ray nuclei from the sun. The surface exposure was for ~ 10,000 years.

Using this energy spectrum and the track density profiles measured in lunar rocks we have obtained an estimate of the rate of fine scale erosion on the moon. Making the necessary corrections for the different properties of the glass and the lunar rocks, for the different solid angles involved, for the solar cycle variation, and assuming the present solar cycle to be typical of the last few million years, we find an erosion rate of 0 to 2 $\times$ 10^{-8} cm/yr to be consistent with the track profiles measured by four groups on rocks 10017 and 10003. The much lower track density profile of rock 10058 is consistent with the recent removal of a chip of appreciable thickness and does not contradict our remarkably low fine-scale erosion rate. Similar results have simultaneously been obtained by CROZAZ and WALKER (1971) and PRICE *et al.* (1971).

Uranium contents and fission track dating

Since fission track dating requires the presence of uranium (PRICE and WALKER, 1963b), the induced fission track measurements given in Table 4 are relevant. In the cases shown, uranium is too low to allow fission track dating of any of the samples except for zircon LZ where an upper limit can be given. Since the fossil track content

Table 4. Uranium content of lunar samples.

Mineral	Sample	Uranium* (wt fraction × 10^9)	Notes
Augite	12017,17,6,3	0.4 (±60%)	Not including visible inclusions
Augite	12017,17,6,3	1.5 (±30%)	Including visible inclusions
Augite	12021,1,4,5	1.0 (±50%)	Not including visible inclusions
Augite	12021,1,4,5	4.5 (±20%)Φ	Including visible inclusions
Augite	12065,6,6	0.5 (±70%)	Including visible inclusions
Glass	12017,8,6	1,230 (±8%)	
Zircon†	LZ (from Apollo 11 fines	167,000 (±12%)	
Zircon†	Z-2 (from Apollo 11 fines)	< 10,000	90% confidence

* Tracks observed on interior surfaces, except as noted.
† Tracks observed in Lexan adjacent to sample.
Φ Most uranium-rich inclusion scanned contained ~ 3 × 10^6 atoms of uranium.

was 1 to 3 × 10^8/cm², the ages would be 1.3 to 3.3 × 10^9 years if these were all fission tracks, and less if an appreciable fraction were of other origin. There is thus no evidence for an excess of fission tracks from presently extinct fission activity by Pu-244 or super-heavy elements.

CONCLUSIONS

Track spallation measurements and solar cosmic ray tracks in the Surveyor III glass add two new dimensions to lunar information available from track measurements. By comparing the spallation and surface residence ages inferred for individual rocks (using spallation and cosmic ray tracks), surface and near surface chronologies can be constructed. By comparing track gradients and abundances in the uneroded glass and in eroded rocks, erosion rates for individual rock surfaces can be determined. Not surprisingly, individual rock histories vary widely.

Acknowledgments—We are pleased to give thanks to H. ALLEN for proton irradiations at the Princeton-Pennsylvania Accelerator, J. FLOYD for neutron irradiation at Brookhaven National Laboratory, U. B. MARVIN of the Smithsonian Astrophysical Observatory for loan of two zircons, to N. NICKLE of the Jet Propulsion Laboratory for Surveyor III glass, and to M. F. CICCARELLI, M. D. MCCONNELL, and E. STELLA for experimental assistance. This work was supported in part by NASA contract NAS 9-7898.

REFERENCES

ALBEE A. L., BURNETT D. S., CHODOS A. A., EUGSTER O. J., HUNEKE J. C., PAPANASTASSIOU D. A., PODOSEK F. A., RUSS PRICE G., II, SANZ H. G., TERA F., and WASSERBURG G. J. (1970) The Lunatic Asylum of the Charles Arms Laboratory of Geological Sciences, *Science*, **167**, 463–466.

ALEXANDER E. C., JR., DAVIS P. K., KAISER W. A., LEWIS R. S., and REYNOLDS J. H. (1971) Depth studies of rare gases in rock 12002. Second Lunar Science Conference (unpublished proceedings).

BAZILEVSKAYA G. A., CHARAKHCYAN A. N., CHARAKYCHYAN T. N., KVASHNIN A. N., PANKRATOV A. K., and STEPANYAN A. A. (1968) The energy spectrum of primary cosmic rays and the secondary radiation background in the vicinity of the earth. *Can. J. Physics*, **46**, S515–S517.

BLOCH M., FECHTIG H., FUNKHOUSER J., GENTNER W., JESSBERGER E., KIRSTEN T., MULLER O., NEUKUM G., SCHNEIDER E., STEINBRUNN F., and ZAHRINGER J. (1971) Location and variation of rare gases in Apollo 12 lunar samples. Second Lunar Science Conference (unpublished proceedings).

CROZAZ G., HAACK U., HAIR M., HOYT P., KARDOS J., MAURETTE M., MIYAJIMA M., SEITZ M., SUN S., WALKER R., WITTELS M., and WOLLUM D. (1970a) Radiation history of the moon. *Science* **167**, 563–566.

CROZAZ G., HAACK U., HAIR M., MAURETTE M., WALKER R., and WOLLUM D. (1970b) Nuclear track studies of ancient solar radiations and dynamic lunar surface processes. *Proc. Apollo 11 Lunar Sci. Conf., Geochim. Cosmochim. Acta* Suppl. 1, Vol. 3, pp. 2051–2080. Pergamon.

CROZAZ G. and WALKER R. M. (1971) Solar particle tracks in glass from the Surveyor III spacecraft. *Science* **171**.

D'AMICO J., DEFELICE J., FIREMAN E. L., JONES C., and SPANNAGEL G. (1971) Tritium and argon radioactivities and their depth variations in Apollo 12 samples. Second Lunar Science Conference (unpublished proceedings).

EBERHARDT P., GEISS J., GRAF H., GROEGLER N., KRAEHENBUEHL U., SCHWALLER H., SCHWARZMUELLER H., and STETTLER A. (1970) Trapped solar wind noble gases, radiation ages and K/Ar in lunar material. *Science* **167**, 558–560.

FIREMAN E. L., D'AMICO J., and DEFELICE J. (1970) Tritium and argon radioactivities in lunar material. *Science* **167**, 566–568.

FLEISCHER R. L., HAINES E. L., HANNEMAN R. E., HART H. R., JR., KASPER J. S., LIFSHIN E., WOODS R. T., and PRICE P. B. (1970a) Particle track, X-ray, and mass spectrometry studies of lunar material from the Sea of Tranquility. *Science* **167**, 568–571.

FLEISCHER R. L., HAINES E. L., HART H. R., JR., WOODS R. T., and COMSTOCK G. M. (1970b) The particle track record of the Sea of Tranquility. *Proc. Apollo 11 Lunar Sci. Conf., Geochim. Cosmochim. Acta* Suppl. 1, Vol. 3, pp. 2103–2120. Pergamon.

FLEISCHER R. L., HART H. R., JR., and COMSTOCK G. M. (1971) Very heavy solar cosmic rays: Energy spectrum and implications for lunar erosion. *Science* **171**, 1240–1242.

FLEISCHER R. L. and PRICE P. B. (1964a) Glass dating by fission fragment tracks. *J. Geophys. Res.* **69**, 331–339.

FLEISCHER R. L. and PRICE P. B. (1964a) Techniques for geological dating of minerals by chemical etching of fission fragment tracks. *Geochim. Cosmochim. Acta* **28**, 1705–1714.

FLEISCHER R. L., PRICE P. B., WALKER R. M., and MAURETTE M. (1967) Origins of fossil-charged particle tracks in meteorites. *J. Geophys. Res.* **72**, 331–353.

FUNKHOUSER J., SCHAEFFER O., BOGARD D., and ZAHRINGER J. (1970) Gas analysis of the lunar surface. *Science* **167**, 561–563.

HINTENBERGER H., WEBER H. W., VOSHAGE H., WANKE H., BEGEMANN F., VILSCEK E., and WLOTZKA F. (1970) Concentrations and isotopic compositions of rare gases, hydrogen, and nitrogen in lunar dust and rocks. *Science* **167**, 543–545.

HONDA M. and ARNOLD J. R. (1964) Effects of cosmic rays on meteorites. *Science* **143**, 203–212.

KOHMAN T. P. and BENDER M. L. (1967) Nuclide production by cosmic rays in meteorites and on the moon. In *High Energy Nuclear Reactions in Astrophysics* (editor B. S. P. Shen) pp. 169–245, Benjamin, Inc.

LAL D., MACDOUGALL D., WILKENING L., and ARRHENIUS G. (1970) Mixing of the lunar regolith and cosmic ray spectra: evidence from particle-track studies. *Proc. Apollo 11 Lunar Sci. Conf., Geochim. Cosmochim. Acta* Suppl. 1, Vol. 3, pp. 2295–2303. Pergamon.

MARTI K., LUGMAIR G. W., and UREY H. C. (1970) Solar wind gases, cosmic-ray effects and the irradiation history. *Science* **167**, 548–550.

MARTI K. and LUGMAIR G. W. (1971) Kr^{81}–Kr and K–Ar^{40} ages, cosmic-ray spallation products and neutron effects in Apollo 11 and Apollo 12 lunar samples. Second Lunar Science Conference (unpublished proceedings).

NAESER C. W. (1969) Etching fission tracks in zircons. *Science* **165**, 388–389.

O'KELLEY D. G., ELDRIDGE J. S., SCHONFELD E., and BELL P. R. (1970) Elemental compositions and ages of Apollo 11 lunar samples by nondestructive gamma-ray spectrometry. *Science* **167**, 580–582.

PRICE P. B., HUTCHEON I., COWSIC R., and BARBER D. J. (1971) Enhanced emission of iron nuclei in solar flares. Second Lunar Science Conference (unpublished proceedings).

PRICE P. B. and O'SULLIVAN D. (1970) Lunar erosion rate and solar flare paleontology. *Proc. Apollo 11 Lunar Sci. Conf., Geochim. Cosmochim. Acta* Suppl. 1, Vol. 3, pp. 2351–2359. Pergamon.

PRICE P. B. and WALKER R. M. (1963a) Fossil tracks of charged particles in mica and the age of minerals. *J. Geophys. Res.* **68**, 4847–4862.

PRICE P. B. and WALKER R. M. (1963b) A simple method of measuring low uranium concentrations in natural crystals. *Appl. Phys. Lett.* **2**, 23–25.

SINTON W. H. (1962) Temperatures on the lunar surface. In *Physics and Astronomy of the Moon* (editor Z. Kupal) pp. 407–428, Academic Press.

STOENNER R. W., LYMAN W. J., and DAVIS R., JR. (1971) Argon and tritium radioactivities in lunar rocks and in the sample return container. Second Lunar Science Conference (unpublished proceedings).

APPENDIX V

Geochim. Cosmochim. Acta, Supplement 2

GENERAL ELECTRIC

REPRINT 6906

GENERAL ELECTRIC COMPANY
CORPORATE RESEARCH AND DEVELOPMENT
P.O. Box 43, Schenectady, N.Y. 12301 U.S.A.

THE PARTICLE TRACK RECORD OF LUNAR SOIL

G.M. Comstock, A.O. Evwaraye,
R.L. Fleischer and H.R. Hart, Jr.

Proceedings of the Second Lunar Science Conference, Vol. 3, pp. 2569–2582
The M.I.T. Press, 1971.

The particle track record of lunar soil

G. M. COMSTOCK, A. O. EVWARAYE,* R. L. FLEISCHER,
and H. R. HART, JR.
General Electric Research and Development Center Schenectady, New York 12301

(*Received* 22 *February* 1971; *accepted in revised form* 29 *March* 1971)

Abstract—Measurements of primary cosmic-ray track densities and spallation-recoil track densities in the Apollo 12 deep-core sample are presented. Neither the primary nor the spallation track densities show any significant dependence on soil depth, while there is a great variation from grain to grain at a given depth. We conclude from this that the soil has been well stirred down to ~60 cm at the Apollo 12 site. This conclusion is quantitatively supported by computer models of the accumulation of cosmic ray tracks in lunar soil. A model in which thorough stirring is most frequent at shallow depths and less and less frequent at greater depths fits the observed track density distributions from both Apollo 11 and Apollo 12 core samples. Stirring ages of at least 1 to 2 billion years are required.

INTRODUCTION

EVIDENCE from manned and unmanned lunar flights that the moon has a deep soil layer or regolith has led to great interest in the origin and mechanical history of this layer. This history has an intimate relationship with lunar surface features and the flux of solid matter in interplanetary space (ÖPIK, 1969, and others). Striking direct evidence for frequent mixing of this soil layer was first provided by fossil particle tracks left in Apollo 11 soil grains by primary heavy cosmic ray nuclei (CROZAZ *et al.*, 1970; FLEISCHER *et al.*, 1970a, b). Further evidence has now been provided by primary cosmic ray and spallation-recoil track densities measured in the Apollo 12 deep core. These results are presented in the following section. We further report the results of Monte Carlo computer calculations which quantitatively support the hypothesis that the particle track distribution is due to frequent mixing of the lunar soil.

APOLLO 12 SOIL SAMPLES

Cosmic ray tracks

We investigated 251 individual pyroxene, feldspar, and olivine soil grains of 50–500 μm diameter from 13 depths distributed through the 40 cm length of the connected core samples 12025 and 12028. These samples were etched and counted in the same manner as described for the Apollo 11 samples (FLEISCHER *et al.*, 1970b).

Primary cosmic ray iron tracks could be counted or lower limits estimated in 73% of the grains sampled (Fig. 1). 61% were counted optically at 1350× magnification. This includes those marked as lower limits, most of which, in fact, probably fall below $\sim 3 \times 10^8/\text{cm}^2$. Transmission electron micrographs of track replicas were made at 7500× for 15% of the samples. Several of these were also counted optically, and the

* Present address: Department of Physics, Antioch College, Yellow Springs, Ohio.

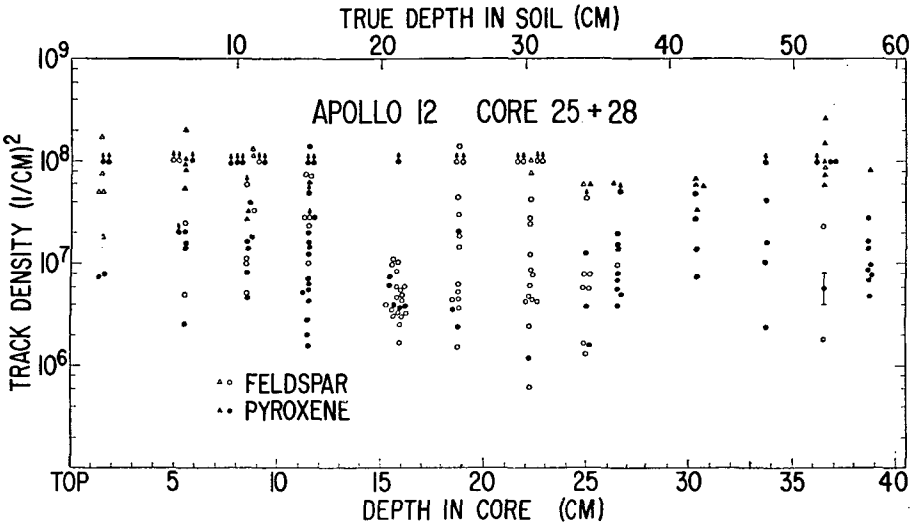

Fig. 1. Cosmic ray track distribution in core 12025 and 12028. The data points are observed optical microscope counts (circles) and adjusted electron micrograph counts (triangles).

micrograph counts were found to be 1 to 3 times greater than the optical counts, depending on track length distribution. The reasons for this have been discussed (FLEISCHER *et al.*, 1970b), and each micrograph count has been reduced by an appropriate factor determined by the track length distribution before inclusion in Fig. 1. No other adjustments were made to the data in Fig. 1.

At least 20% of the samples that were counted contained track gradients (for example, Fig. 3 of FLEISCHER *et al.*, 1971). In these cases, the counts were made from near the center of the grains; track densities near certain edges are often more than 10 times greater.

The statistical counting error for each sample is generally less than 10%. The error bars shown in Figs. 1, 2, and 3 represent the spread in counts obtained when larger samples were broken up and the fragments counted separately. The observed factor of 2 spread could arise from variations in etching efficiency and random orientation of the etched surface with respect to the cosmic ray flux.

The 40 cm length of the core is in fact sampling the top 60 cm of soil (CARRIER *et al.*, 1971). It is clear (Fig. 1) that there is a real spread in track densities of at least a factor of 100 at most depths and that there is no systematic decrease in track density with depth down to 60 cm. We did not obtain samples from the so-called gravel layer at soil depth 15–20 cm which has a low track density (CROZAZ *et al.*, 1971; BHANDARI *et al.*, 1971). Our samples at about 20 cm (Fig. 1) may be related to this layer.

The 27% of the grains sampled which are not included in Fig. 1 became rapidly overetched to a partially opaque condition which often, but not always, indicates a high track density. These may represent an additional high density population, so

that at least 14% and possibly as much as 40% of the soil grains have $>10^8$ tracks/cm^2. BHANDARI *et al.* (1971) report that 45% of the soil samples have $>10^8$ tracks/cm^2. However, BARBER *et al.* (1971a) and CROZAZ *et al.* (1971) report a much higher fraction (80–90%) with $>10^8$ tracks/cm^2. Part of this discrepancy results from a lack of standardization: CROZAZ *et al.* (1970, 1971) are referring to deep pits viewed with the scanning electron microscope, which can reveal a density twice as great as the same region viewed optically. However, a real effect may exist, related to sample selection or track identification. Correlation with size is suggested by micron-size soil grains observed to have very high track densities (BORG *et al.*, 1971; BARBER *et al.*, 1971b). More detailed comparison of the various techniques used is necessary to clarify this situation.

Spallation tracks

In addition to primary cosmic ray tracks, the lunar soil grains also contain recoil tracks of heavy spallation products from high energy cosmic ray collisions with constituents of the minerals (FLEISCHER *et al.*, 1970a). These tracks are much shorter than the cosmic ray iron tracks. They are clearly visible on micrographs of plastic replicas but tend to be obscured when regions of high cosmic-ray-track densities are etched sufficiently to reveal them optically.

We sought spallation tracks in 85 grains which had cosmic ray track densities $\lesssim 3 \times 10^7$ cm^{-2} (optically visible at 1000×). The spallation track density is defined here to be the number of dots visible under reflected light minus the number of (cosmic ray) tracks with finite length under transmitted light.

Counts were obtained in this way from 80% of the grains sampled (Fig. 2). An additional 8% had no visible spallation tracks. Either these were not sufficiently etched, had a concentration $<10^6$ cm^{-2}, or were of an orientation with a low etching efficiency. Surface features could not be resolved under reflected light in 12% of the samples and this could be due to spallation track densities $\gtrsim 5 \times 10^7$ cm^{-2}. We see no significant variation with depth and a spread at each depth of a factor of $\sim$10.

There is no apparent correlation between cosmic ray and spallation track densities (Fig. 3). Those samples with cosmic ray gradients have been closer to the surface and so are displaced toward higher cosmic ray track densities; however, their spread in spallation counts is the same as samples without gradients. This gives us confidence that we are interpreting the spallation tracks properly and that samples with high cosmic-ray track density might tentatively be assumed to exhibit the same spallation distribution (cross-hatched region in Fig. 3).

Soil models

We now consider what these results can tell us about lunar soil history. The discussion is based on the depth dependence of the cosmic ray and spallation track production rates. The cosmic ray tracks are due almost entirely to primary iron nuclei. The flux of these particles is very high near the surface but falls off rapidly with depth due to a decreasing energy spectrum and an interaction mean path (in lunar soil) of 12 cm. Lighter cosmic ray nuclei are much more penetrating, however,

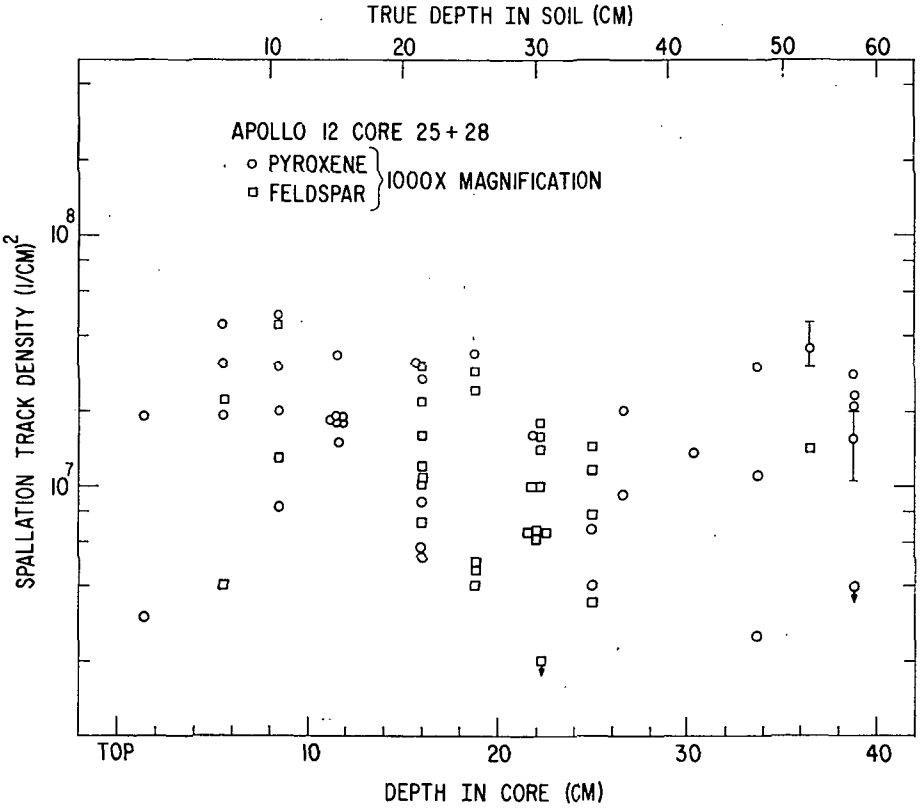

Fig. 2. Spallation-recoil track distribution in core 12025 and 12028. All data are optical microscope counts.

and the spallation track production rate shows a very different behavior. It first increases with depth due to the cosmic ray-induced production of secondaries which in turn induce spallation recoils. For the spallation products which are most likely to leave tracks, the production rate increases by a factor of ~2 from the surface down to 20–25 cm where it reaches a maximum (KOHMAN *et al.*, 1967).

By comparing these growth rates with the observed track distributions, we can learn about the mechanical history of the soil. We consider here three basic models of soil movement. First, a *quiet soil* model in which the individual soil grains have suffered no appreciable change of depth. In this case the track distributions should be proportional to the track production curves. The cosmic ray track density spread at any particular depth should be a factor of ~2 due to random orientation of the etched surface with respect to the attenuated cosmic ray flux. A similar spread for spallation tracks can be expected from variations in etching efficiency (FLEISCHER *et al.*, 1971). The quiet soil case is illustrated for cosmic ray iron tracks in Fig. 4,

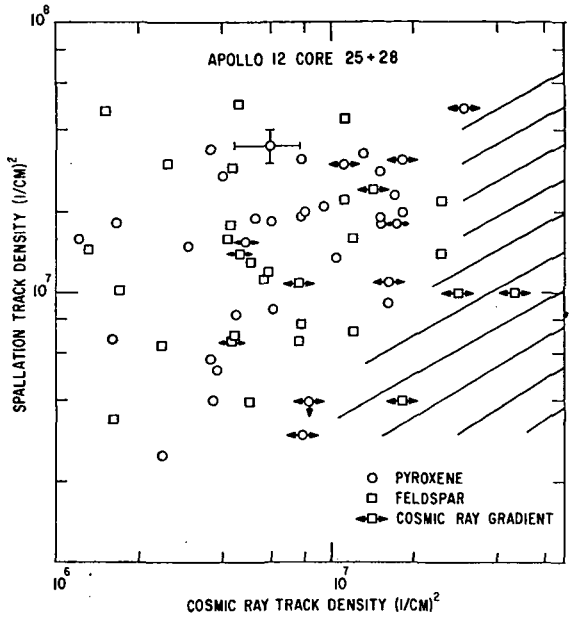

Fig. 3. Correlation between cosmic ray and spallation tracks. Spallation track densities were not measured in the cross-hatched region.

where the curve marked "no mixing" refers to the quiet soil model after 1 billion years.

We have also plotted in Fig. 4 the median track density observed at each depth with limit bars that show the spread of the 70% of the samples closest to the median. The quiet soil model clearly does not satisfy the observed distribution. The spallation track distribution (Fig. 2) also has too much variation at each depth and does not show a depth dependence proportional to the production rate. A lack of correlation between cosmic ray and spallation tracks is also expected if the grains have not spent most of their time at the same depth.

Second, we consider a *burial model* in which an initially trackless soil experiences a steady burial, with relatively insignificant mixing (e.g. BHANDARI *et al.*, 1971). In this case, the track density expected at a given depth is (for uniform burial) the integral of the production function from some initial depth to the observed depth. The cosmic ray track density would increase rapidly in the first ~1 cm and approach an essentially constant value below that depth, an observation which is consistent with the observed median values (Fig. 4). We cannot state definitely what spread in track density at a given depth would be expected from this model without specifying the burial mechanism. The distribution of initial surface depths is critical; for example, a wide spread could come from tracks formed while the samples were still part of surface rocks and thus shielded to varying degrees.

The spallation track density, however, would continue to increase strongly throughout the depths sampled as a grain is buried. This is not what is observed (Fig. 2).

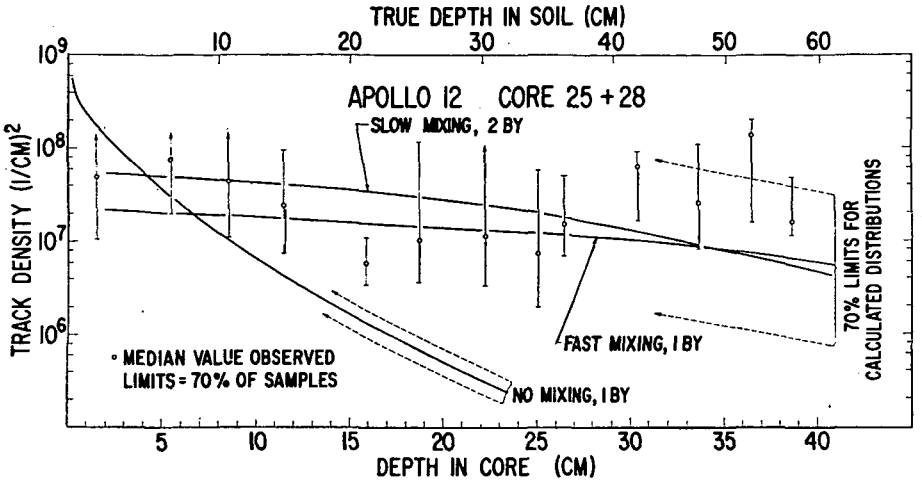

Fig. 4. Cosmic ray track distribution in core 12025 and 12028. The data points are derived from optical and (adjusted) electron microscope counts. The curves have been calculated for some of the models of soil history described in the text.

On the basis of the spallation tracks, therefore, we conclude that a burial model is not sufficient as long as the burial process involves layers that contain few spallation tracks when deposited. Preburial exposure of the grains (e.g. while in their parent rock) may weaken this conclusion.

Finally we consider *mixing models* which postulate that the major contribution to soil movement is frequent mixing by depth-dependent excavation and overlay of soil predominantly caused by small impact events. This model and a computer simulation are discussed in more detail in the following section, but the basic properties expected for cosmic ray iron tracks are indicated in Fig. 4 for two mixing rates. The "slow mixing" is derived from the maria crater distribution function (SHOEMAKER *et al.*, 1970); "fast mixing" uses a mixing rate ten times faster. The curves give calculated median values with the spread of 70% of the distribution as indicated, in good agreement with the data points. The spread in cosmic ray track densities in the mixing model is due to the distribution of residence times at depths $\leqslant 20$ cm. The interpretation of layering in this model is discussed in the following section.

In this model, mixing of the top meter or so of soil would also produce an essentially depth-independent distribution of spallation tracks, as observed, with a spread at each depth reflecting the variation of production rate over the range of depths mixed, perhaps a factor of ~ 10.

The basic features of these models and the observations are summarized in Table 1.

LUNAR SOIL MIXING

Physical process

We now specify the mixing model favored by the evidence discussed in the last section.

Table 1. *Lunar soil models.*

Model	Track Source	Track density vs. depth above 60 cm	Spread at each depth	Cosmic ray-spallation correlation
Quiet soil	Cosmic ray Fe	Decreasing	$\sim \times 2$*	Strong correlation
	Spallation	Peaks at $\approx$25 cm	$\sim \times 2$*	
Frequent overlaying, sub-cm mixing only	Cosmic ray Fe	$\sim$Constant	$> \times 100$?†	None
	Spallation	Increasing	$\sim \times 2$*	
Frequent depth-dependent turnover	Cosmic ray Fe	$\sim$Constant	$\sim \times 100$‡	None
	Spallation	$\sim$Constant	$\sim \times 10$§	
Apollo 12 core observations	Cosmic ray Fe	$\sim$Constant	$\geq \times 100$	None
	Spallation	$\sim$Constant	$\geq \times 10$	

* Due primarily to random orientation of etched surface.
† Due to distribution of depths in overlay and broken rocks.
‡ Due to distribution of residence times at depths $\leq$20 cm.
§ Due to variation of production rate over range of mixed depths.

Theoretical analyses of surface activity generated by impact events have been made, for example, by ÖPIK (1969) and references therein. SHOEMAKER *et al.* (1970) have discussed the nature of the soil layer, or regolith, of Mare Tranquillitatus (landing site of Apollo 11). Experimental studies, such as GAULT *et al.* (1966) have been made of impact cratering mechanics. The physical processes indicated by such studies can be summarized as follows. Impact on the lunar surface by meteoroids causes soil and rock to be excavated from a crater and deposited on the surface in a blanket extending $\sim$2 crater diameters, with some material thrown much greater distances. Material thrown out of nearby craters will in turn overlay and bury this until excavation occurs again. After a given period of time the statistical nature of this activity will cause the soil layer to be completely turned over down to a certain median depth; during this time, the depth history of a particular soil grain will be quite complicated.

From the size-frequency distribution of craters observed at Mare Tranquillitatus, SHOEMAKER *et al.* (1970) have derived the time t required for turnover down to a median depth d ($\leq$10 cm) to be approximately $t = 0.0025Ad$ where A is the age of the mare surface. For $A = 4$ b.y. this gives t (m.y.) $= 10d$ (cm); since the cratering rate might have been greater in the past, we also consider here the effect of a model using t (m.y.) $= d$ (cm).

This near-surface stirring will be due primarily to events which produce craters $\leq$5 m in diameter. It is known that craters this small will disappear by erosion, overlay, and obliteration by larger craters in a lifetime small compared to the age of the maria. On this scale, the mare surface is said to be in equilibrium. In fact, many if not most of the craters which contribute to turning over the soil to a given depth d will disappear in the turnover time t, which is simply a restatement of the complicated excavation and burial history of a given soil grain over one mixing time.

Computational model and interpretation

We will be comparing this model to core sites where no large cratering event has occurred recently, so that the above discussion applies. It follows that for these sites we can assume that a large number of samples distributed randomly down to the

mixing depth $d \leqslant 1$ m will again be distributed randomly after one mixing time. The present computations use this property to approximate the detailed depth history of a soil grain. We assume that periodic mixes down to three different mixing depths dc are characteristic of the near-surface stirring process in the following manner.

For the lower mixing rate described above we start with 1800 hypothetical samples distributed through the top 60 cm of soil. Every 100 m.y. (one mixing time for $dc = 10$ cm) those samples which have depths of 0–10 cm are assigned new depths at random between 0–10 cm. Similarly samples 0–25 cm deep and 0–60 cm deep are assigned new depths every 250 m.y. and 600 m.y., respectively. At each such "characteristic mix" we keep account of the accumulated tracks except for 1% of the samples mixed which are reassigned 0 track density to simulate shock and impact-heat annealing (this is roughly the fraction of glass observed divided by the number of characteristic mixes over 4 b.y.). For the faster rate we mix depths of 0–10 cm, 0–30 cm, and 0–100 cm every 10, 30, and 100 m.y., respectively.

This model is designed to demonstrate the effects of periodically bringing material up from lower depths and of mixing the shallow depths more frequently. The characteristic mixes do not correspond to individual cratering events but simulate in one process the physically separate events of repeated excavation and burial by overlaying. The nature of these separate events is such that we would expect this computational model to underestimate the number of samples which spend time within a few hundred microns of the surface; i.e. to underestimate the high density tail of the track density distribution.

Next we consider the effect of mixing deeper than one meter, not included in the computations just described. Sample grains which remain below 1 m will acquire essentially no primary tracks. Nearby deep cratering events will lay down a blanket of such samples around a soil core site; if the blanket is deeper than the core sample, it will essentially restart the process of track accumulation. The annealing caused by deposits of lava and volcanic ash will have the same effect. We, therefore, start our computations with no tracks and interpret the derived cosmic ray age as the time since the last deep-cratering or track-annealing event in the vicinity of the core site. Since only a few such events have occurred at a given site, we expect this time to be long. Such an event might also lay down a shallower layer of trackless material. If subsequent mixing has not had time to obliterate such a layer, then soil grains below will record mixing history before the event.

Note that grains brought near the surface for the first time may physically be part of rocks (freshly broken from bedrock) which presumably are not as susceptible to burial and shallow mixing as the smaller soil grains. However, measured surface residence times (CROZAZ *et al.*, 1970; FLEISCHER *et al.*, 1970b) and predicted destruction times (SHOEMAKER *et al.*, 1970) indicate that such rocks are relatively quickly broken up and so should have little effect on the subsequent mixing history.

Track growth rate

As the mixing process described above evolves with time, the hypothetical samples accumulate tracks at a depth-dependent rate determined from the average primary

cosmic ray spectrum. Primary particle tracks in lunar soil are due mostly to high-energy cosmic ray iron nuclei. The energy spectrum of these nuclei has been measured in interplanetary space by COMSTOCK *et al.* (1969) and extrapolated from balloon observations (FREIER and WADDINGTON, 1968). This solar-modulated energy spectrum (observed at the minimum of solar activity) has been corrected to the average level over the 11-year solar cycle using a model by WANG (1970). Observations in meteorites of primary particle tracks (FLEISCHER *et al.*, 1967) and spallation products (HONDA and ARNOLD, 1964) support the assumption that this average spectrum has been roughly constant in the geologic past. From this energy spectrum, taking into account particle range and loss of iron nuclei by spallation in lunar material, distribution of path lengths in a semi-infinite soil, and etching characteristics of the soil minerals, we calculate the rate of track accumulation at a given depth. The track density per area is assumed to be observed in a plane parallel to the surface.

Results

Some of the results of these calculations are shown in Fig. 5. This figure shows the distribution of etched track densities after 2.8 b.y. for the samples in two depth intervals: the top 10.5 cm, corresponding to the Apollo 11 core depth, and the 30 to 40 cm interval, to compare with the Apollo 12 deep core. The scale is logarithmic, by factors of 2.

In this case the top 10 cm are mixed every 100 m.y., the top 25 cm every 250 m.y. and the top 60 cm every 600 m.y. For times earlier than about 2 b.y. the distributions at the two depths vary greatly from each other, with the top 10 cm initially acquiring tracks at a much higher rate. After ~2.5 b.y. the soil approaches uniformity down to a half meter, the distributions becoming very similar at different depths. At all later times each depth acquires tracks at the same average rate because of the frequent mixing.

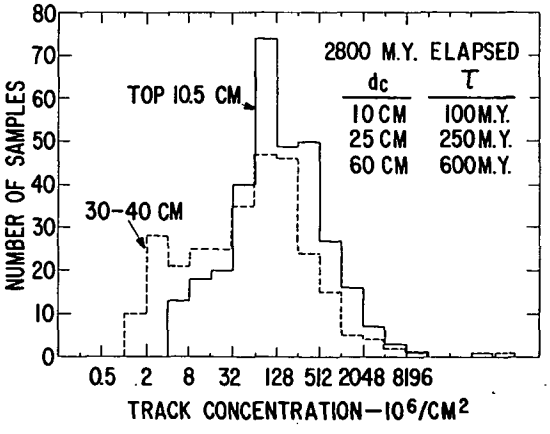

Fig. 5. Calculated distributions of track density in two depth intervals after 2.8 b.y. of soil mixing. The samples were periodically mixed down to three characteristic depths dc with time periods τ.

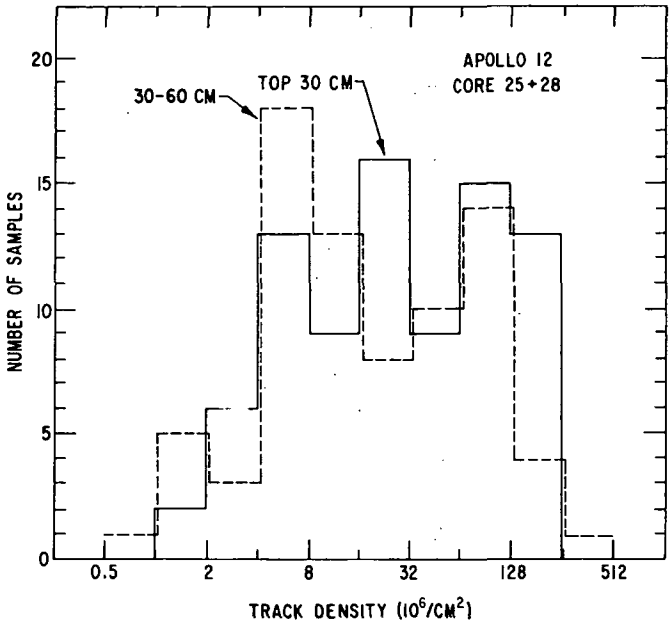

Fig. 6. Observed frequency distributions of track density in core 12025 and 12028 summed over two soil-depth intervals, 0–30 cm (solid line) and 30–60 cm (dashed line). The 0–30 cm distribution does not include the data from a possible special layer at ≈16 cm (Fig. 1). Lower limits have been smoothed over the next factor of 4.

The observed track density vs. frequency distribution summed over depth is shown in Fig. 6 for Apollo 12. The top half (0–30 cm) and bottom half (30–60 cm) of core 12025 + 12028 are summed separately to display any systematic change with depth. The samples at ≈16 cm (Fig. 1) were omitted since they may represent a layer that is not well mixed, as discussed later. Samples with lower limits (Fig. 1) have been smoothed over the next higher factor of 4; some of these may have still higher densities. Figure 7 shows the track density distribution observed in Apollo 11 core 10005. The track density shown in Figs. 6 and 7 should be increased by a factor of ~2 to correct for the random orientation of the etched crystal surface with respect to the cosmic ray flux. The distributions are similar to that shown in Fig. 5, both in absolute track density and in spread.

The time history of the calculated model is made clear in Fig. 8. Here we have plotted the medians of the calculated distributions as a function of time, as the system evolves, for two depth intervals. The arrows indicate the times and depths of the characteristic mixes used. The sharp breaks in the curves are due to the effects of the assumed mixes; in a real physical situation, the curves would have a much more irregular appearance. However, the envelopes of the model curves are meaningful and the approach to uniformity with depth at later times is clear. On the basis of the Apollo 11 results alone, in the top 10.5 cm, and for the mixing rate assumed, we could only conclude that the exposure age of the mixed soil is at least ~500 m.y.

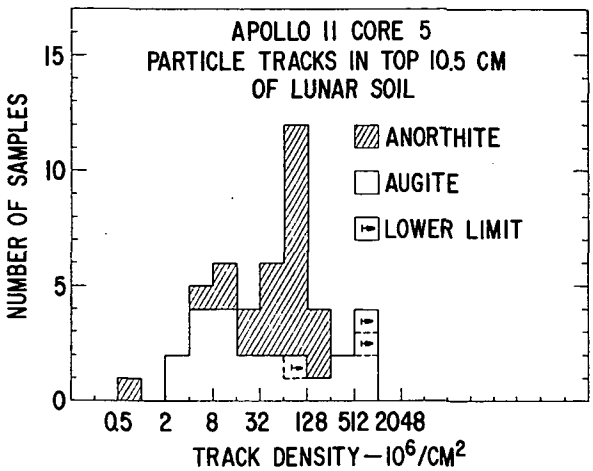

Fig. 7. Observed frequency distribution of track density for samples from throughout the top 10.5 cm of soil at Tranquillity Base. Each sample is a different soil grain. For comparison with Figs. 5, 8, and 9 these track densities should be increased by an average factor of 2 to correct for random orientation of the etched crystal surface.

On the basis of the deeper Apollo 12 core we can push this lower age limit up to about 2 b.y.

As indicated earlier, the average mixing rate is uncertain, and we also have investigated a faster mixing rate, shown in Fig. 9. Here the track densities approach uniformity much faster and the lower age limit is about 1 b.y. for the Apollo 12 site.

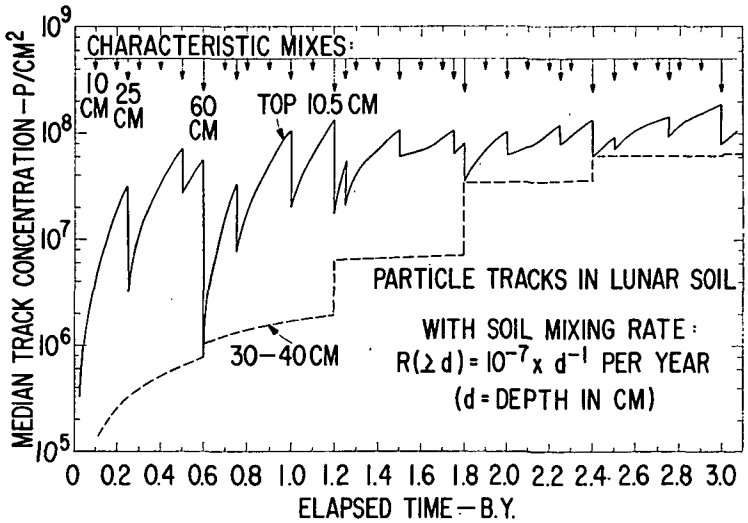

Fig. 8. Time history of the median value of the track density distributions for two depth intervals, 0–10 cm (solid line) and 30–40 cm (dashed line). Times and depths of the characteristic mixes used are also shown. A soil grain at depth d is mixed with rate $R(\geqslant d)$.

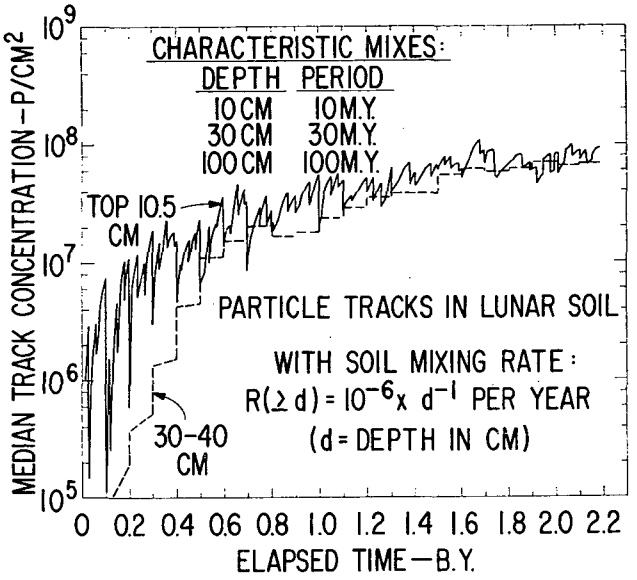

Fig. 9. Time history of the median value of the track density distributions for two depth intervals, 0–10 cm (solid line) and 30–40 cm (dashed line), for a fast mixing rate. Somewhat deeper characteristic mixing depths are used in this case.

When the results of these calculations are adjusted for average orientation and plotted vs. depth, we obtain the curves in Fig. 4 discussed in the preceding section.

Layers and surface residence

The mixing model discussed here does not contradict the existence of some layering. In this picture, the reported gravel layer at $\approx$13 cm and possibly the low-track-density samples at $\approx$16 cm are the bottom remnants of a fresh blanket brought up from $\approx$1 m, laid down over well-mixed soil and not yet completely obliterated. This blanket has since been covered by, and partially mixed with, other well-stirred soil; eventually it may be completely destroyed. The existence of such layers indicates the discrete nature of the excavation and overlay events which make up the mixing process and can be important in studying the details of this process.

Of equal importance is the occurrence of very high-track densities resulting from surface residence. We have indicated that this region is uncertain experimentally, and that the present computer model is probably underestimating the high density contribution. The role of high track densities needs to be studied further.

CONCLUSIONS

The distribution of cosmic ray and spallation-recoil tracks in the Apollo 12 deep core allow us to choose among three basic models for the lunar soil as summarized in Table 1. The evidence shows conclusively that the soil is not quiet and undisturbed.

The spallation tracks imply that simple burial by overlay or surface transport is not enough but rather that at least the top meter of soil has been subjected to mixing. Computer simulation of frequent soil turnover agrees well with the cosmic-ray track distribution and requires stirring times of at least 1 to 2 b.y. since the last cratering event large enough to lay down a deep blanket of material from well below 60 cm.

This mixing process involves discrete excavation and overlay events, and hence some temporary structure, due to shallow layers of previously deep material, might be expected to persist for a time. Detailed track studies of such structure and of deeper core samples would tell us more about the stirring mechanism and help to unravel the history of larger-scale ground movement such as the slumping of crater walls and rille formation.

Acknowledgments—We are pleased to acknowledge the able experimental assistance of E. F. KOCH, M. D. MCCONNELL, and E. STELLA. This work was supported in part by NASA under contract NAS 9-7898.

REFERENCES

ARRHENIUS G., ASUNMAA S. K., LIANG S., MACDOUGALL D., WILKENING L. (1971) Irradiation and impact in Apollo rock and soil samples. Second Lunar Science Conference (unpublished proceedings).

BARBER D. J., HUTCHEON I. D., PRICE P. B., RAJAN R. S., and WENK R. (1971a) Exotic particle tracks and lunar history. Second Lunar Science Conference (unpublished proceedings).

BARBER D. J., HUTCHEON I. and PRICE P. B. (1971b) Extralunar dust in Apollo cores? *Science* **171**, 372–374.

BHANDARI N., BHAT S., LAI D., RAJAGOPALAN G., TAMHANE A. S., and VENKATAVARADAN V. S. (1971) Fossil track studies in lunar material. II: The near-surface exposure history of regolith components. Second Lunar Science Conference (unpublished proceedings).

BORG J., DURRIEU L., DRAN J. C., JOURET C., and MAURETTE M. (1971) Irradiation, texture, and habit histories of the lunar dust grains. Second Lunar Science Conference (unpublished proceedings).

CARRIER W. D., III, JOHNSON S. W., WERNER R. A., and SCHMIDT R. (1971) Distortion in samples recovered with the Apollo core tubes. Second Lunar Science Conference (unpublished proceedings).

COMSTOCK G. M., FAN C. Y., and SIMPSON J. A. (1969) Energy spectra and abundances of the cosmic ray nuclei helium to iron from the OGO-1 satellite experiment. *Astrophys. J.* **155**, 609–617.

CROZAZ G., HAACK U., HAIR M., MAURETTE M., WALKER R., and WOOLUM D. (1970) Nuclear track studies of ancient solar radiations and dynamic lunar surface processes. *Proc. Apollo 11 Lunar Science Conf., Geochim. Cosmochim. Acta*, Suppl. 1, Vol. 3, pp. 2051–2080. Pergamon.

CROZAZ G., WALKER R., and WOOLUM D. (1971) Solar and galactic cosmic ray studies in fines and rocks. Second Lunar Science Conference (unpublished proceedings).

FLEISCHER R. L., PRICE P. B., WALKER R. M., MAURETTE M., and MORGAN G. (1967) Tracks of heavy primary cosmic rays in meteorites. *J. Geophys. Res.* **72**, 355–366.

FLEISCHER R. L., HAINES E. L., HANNEMAN R. E., HART H. R., JR., KASPER J. S., LIFSHIN E., WOODS R. T., and PRICE P. B. (1970a) Particle track, X-ray and mass spectrometry studies of lunar material from the Sea of Tranquillity. *Science* **167**, 568–571.

FLEISCHER R. L., HAINES E. L., HART H. R., JR., WOODS R. T., and COMSTOCK G. M. (1970b) The particle track record of the Sea of Tranquillity. *Proc. Apollo 11 Lunar Science Conf., Geochim. Cosmochim. Acta*, Suppl. 1, Vol. 3, pp. 2103–2120. Pergamon.

FLEISCHER R. L., HART H. R., JR., COMSTOCK G. M., and EVWARAYE A. O. (1971) Particle track record of the Ocean of Storms. Second Lunar Science Conference (unpublished proceedings).

FREIER P. S. and WADDINGTON C. J. (1968) Very heavy nuclei in the primary cosmic radiation. I. Observations of the energy spectrum. *Phys. Rev.* **175**, 1641–1648.

GAULT D. E., QUAIDE W. L., and OBERBECK V. R. (1968) Impacet cratering mechanics and structures. *Proc. Conf. on Shock Metamorphism of Natural Materials*, pp. 87–99. Mono Book, Baltimore.

HONDA M. and ARNOLD J. R. (1964) Effects of cosmic rays on meteorites. *Science* **143**, 203–212.

KOHMAN T. D. and BENDER M. L. (1967) Nuclide production by cosmic rays in meteorites and on the moon. In *High Energy Nuclear Reactions in Astrophysics* (Editor, B. S. P. SHEN), pp. 169–245. Benjamin.

LAL D., MACDOUGALL D., WILKENING L., and ARRHENIUS G. (1970). Mixing of the lunar regolith and cosmic ray spectra: Evidence from particle-track studies. *Proc. Apollo 11 Lunar Science Conf., Geochim. Cosmochim. Acta*, Suppl. 1, Vol. 3, pp. 2103–2120. Pergamon.

ÖPIK ERNST J. (1969) The moon's surface, in *Annual Review of Astronomy and Astrophysics* **7**, 473–526. Annual Reviews, Inc. Palo Alto, California.

PRICE P. B. and O'SULLIVAN D. (1970) Lunar erosion rate and solar flare paleontology. *Proc. Apollo 11 Lunar Science Conf., Geochim. Cosmochim. Acta*, Suppl. 1, Vol. 3, pp. 2351–2359. Pergamon.

SHOEMAKER, E. M., HAIT M. H., SWANN G. A., SCHLEICHER D. L., SCHABER G G., SUTTON R. L., DAHLEM D. H., GODDARD E. N., and WATERS A. C. (1970) Origin of the lunar regolith at Tranquillity Base. *Proc. Apollo 11 Lunar Science Conf., Geochim. Cosmochim. Acta*, Suppl. 1, Vol. 3, pp. 2399–2412. Pergamon.

WANG J. R. (1970) Dynamics of the 11-year modulation of galactic cosmic rays. *Astrophys. J.* **160**, 261–281.

APPENDIX VI

Proceedings, I.A.U. Symposium #47, "The Moon", Newcastle-upon-Tyne (to be published)

GENERAL ELECTRIC

GENERAL ELECTRIC COMPANY
CORPORATE RESEARCH AND DEVELOPMENT
Schenectady, N.Y.

THE PARTICLE TRACK RECORD OF THE LUNAR SURFACE

by

G. M. Comstock, General Physics Laboratory

Report No. 71-C-190 June 1971

TECHNICAL INFORMATION SERIES

CLASS 1

GENERAL ELECTRIC

General Electric Company
Corporate Research and Development
Schenectady, New York

TECHNICAL INFORMATION SERIES

AUTHOR	SUBJECT	NO. 71-C-190
Comstock, GM	moon	DATE June 1971
TITLE The Particle Track Record of the Lunar Surface		GE CLASS 1
		NO. PAGES 13
ORIGINATING COMPONENT General Physics Laboratory		CORPORATE RESEARCH AND DEVELOPMENT SCHENECTADY, N.Y.

SUMMARY Information about lunar surface history revealed by fossil particle tracks is summarized. Such tracks are the result of damage left in dielectric materials by highly ionizing charged particles including heavy solar and galactic cosmic ray nuclei, heavy nuclei recoiling from cosmic ray induced spallation reactions, and induced- and spontaneous-fission fragments. From the distribution of cosmic ray and spallation tracks in the lunar rock, surface residence times of 1 to 30 million years and rock erosion rates of 1Å to 10Å per year have been determined. Particle tracks also record surface orientation and depth history of the rocks and contain information about ancient solar activity. The distribution of particle tracks in lunar soil is found to be consistent with a model which includes repeated excavation, layering, and burial. With this model, one-core-12025+28 soil layer can be identified as unmixed and weakly irradiated; the others contain soil which has been better and better mixed and more and more irradiated.

KEY WORDS

moon, particle tracks, cosmic rays, micrometeorites

INFORMATION PREPARED FOR _____

_____

Additional Hard Copies Available From

Corporate Research & Development Distribution
P.O. Box 43 Bldg. 5, Schenectady, N.Y., 12301

Microfiche Copies Available From

Technical Information Exchange
P.O. Box 43 Bldg. 5, Schenectady, N.Y., 12301

RD-54 (10/70)

THE PARTICLE TRACK RECORD OF THE LUNAR SURFACE*

G. M. Comstock

INTRODUCTION

The study of fossil particle tracks in lunar material has yielded much information concerning the history of lunar rocks and soil as well as ancient levels of energetic particle fluxes (Barber et al., 1971a, b; Bhandari et al., 1971a, b; Borg et al., 1971a, b; Comstock et al., 1971; Crozaz et al., 1970, 1971; Fleischer et al., 1970b, c, 1971a, b; Lal et al., 1970; Price et al., 1970b, 1971).

In this report we summarize some of the results of particle track studies in lunar materials, and develop further the conclusions that can be drawn from track densities in soil grains. We first summarize briefly the possible sources of lunar particle tracks. The production rates of cosmic ray and spallation tracks are then discussed and interpretation in terms of rock exposure ages and erosion rates are summarized. The last part of the report is devoted to a discussion of the layering, mixing, and irradiation history of the soil, based on the track distributions observed in the Apollo 12 double core.

SOURCES OF LUNAR PARTICLE TRACKS

Fossil particle tracks mark the damaged region left in dielectric materials by the passage of highly ionizing charged particles. If the particles are sufficiently ionizing they cause permanent disruptions of the lattice structure (Fleischer et al., 1967). Laboratory evidence (Fleischer et al., 1970d) indicates that in lunar crystals the annealing or erasure of tracks due to temperatures normally experienced on the moon can be considered negligible. When introduced to the proper chemical etchant the damaged tracks can etch faster than the general surface resulting in a cone-shaped cavity. For a given etching time the shape of the cone depends on the charge and energy of the incident particle; in particular, the cone length depends strongly on the rate of primary ionization (Price et al., 1967).

In a given material there is an ionization rate, or registration threshold, below which there will not be sufficient damage to result in an etchable track. In lunar materials this threshold allows the registration of nuclei heavier than Z ~20 (calcium) (Plieninger and Krätschmer, 1971). These nuclei are therefore observable over that portion of their range where the rate of primary ionization exceeds the registration threshold.

In Table I we have listed the possible sources of particles capable of leaving etchable tracks in lunar material. This list also applies to meteorites for which many of the techniques used to study particle tracks were developed (Fleischer et al., 1967). Monopoles, if they exist (Fleischer et al., 1970a), would have to leave tracks $\gtrsim 1/2$ cm long in order not to be confused with the heaviest cosmic ray tracks (Fleischer et al., 1967; Barber et al., 1971a).

TABLE I

Possible Sources of Tracks on the Moon

1. Cosmic Ray Tracks - Solar and galactic nuclei with charge Z>20-23.
2. Spallation Tracks - Heavy nuclei recoiling from spallation reactions induced by primary and secondary cosmic ray protons, neutrons and alpha particles.
3. Fission Tracks - Fragments from spontaneous fission of U^{238}, Pu^{244} and possibly superheavy elements.
4. Induced Fission Tracks - Fission induced by cosmic ray protons on Pb, Th, or U or by secondary neutrons.

Also -

5. Meson jets induced by very high energy cosmic rays (rare).
6. Dirac monopoles (hypothetical).

Spontaneous and cosmic-ray-induced fission tracks are important constituents of particle tracks on the moon, although the only reported cosmic-ray-induced fission events are those found in a sample of lead-bearing filter glass that was part of the *Surveyor III spacecraft* (Fleischer et al., 1971b). The study of spontaneous fission tracks in terrestrial materials has led to the very fruitful field of fission-track dating (reviewed by Fleischer and Hart, 1970d).

On the moon, however, fission track densities are generally much less than cosmic ray and spallation track densities except in certain uranium-rich minerals (Burnett et al., 1971) and perhaps at great depths (which have been shielded from cosmic rays). Lunar fission tracks can be studied by mapping uranium-rich inclusions (Crozaz et al., 1970; Fleischer et al., 1970c) or by investigating excess track densities along crystal cleavages which often represent grain boundaries where heavy elements concentrate (Bhandari et al., 1971b). Bhandari et al. report that these excess tracks tend to be

* This work was supported in part by NASA under Contract NAS 9-7898.

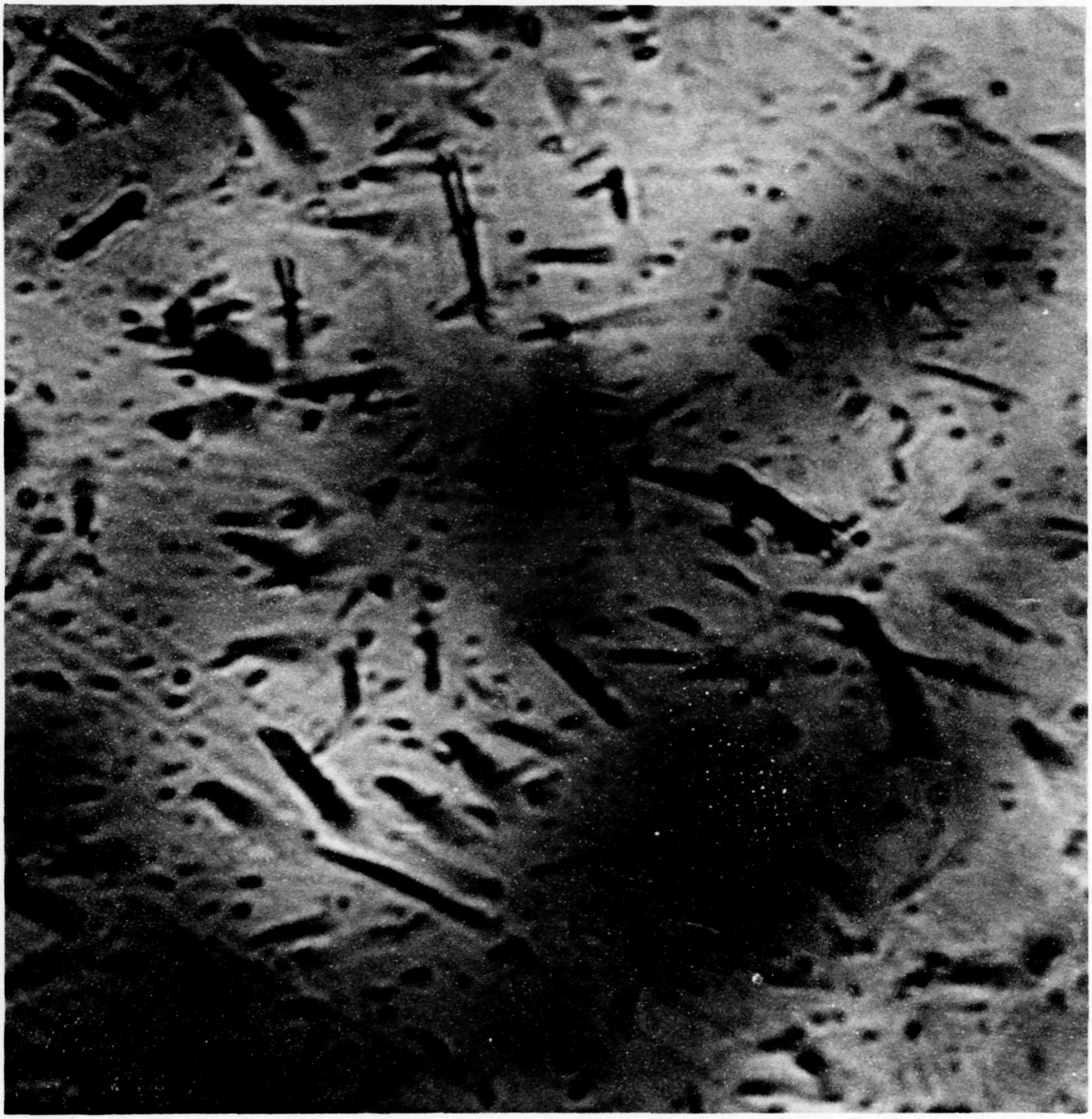

Fig. 1 Optical photograph of cosmic ray tracks (comet-shaped) and spallation tracks (dots) in a lunar crystal.

longer (13 to 25 μm) than the abundant iron tracks (10 to 13 μm) and interpret the longer tracks as fission tracks. These authors interpret their results as evidence for the primordial existance of Pu^{244} and possibly of superheavy elements.

By far the most abundant particle tracks on the moon are the cosmic ray and spallation recoil tracks (as used here the term cosmic ray includes solar as well as extra-solar or galactic particles). An optical photograph (transmitted light) of a sample of these tracks is shown in Fig. 1. The long comet-shaped objects--cosmic ray tracks, $\lesssim$11 μm--were produced primarily by cosmic ray iron nuclei, the most abundant species which will register tracks. Their density here is only a few million per cm^2 which is relatively low for lunar material. The dots--spallation tracks--are very short tracks left by heavy nuclei recoiling from cosmic-ray-induced spallation reactions.

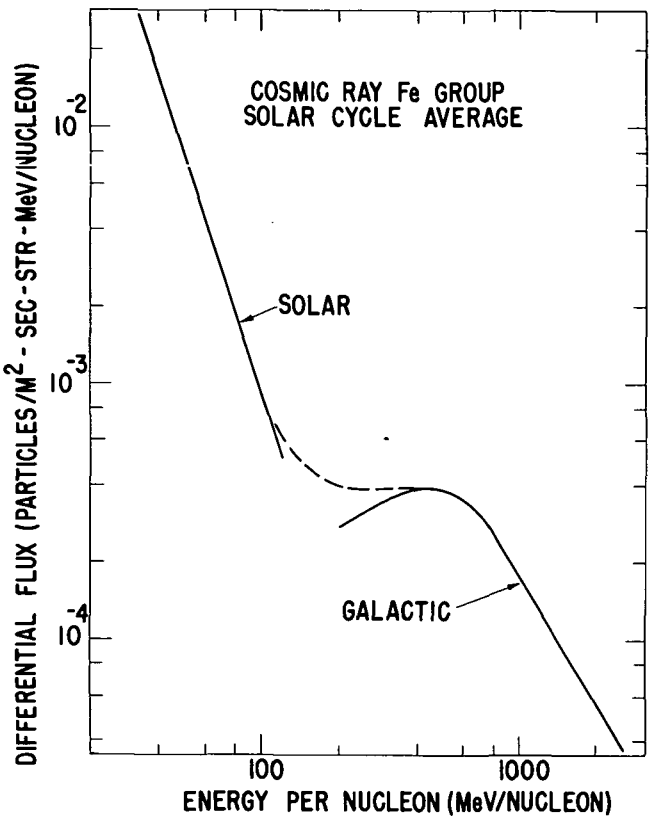

Fig. 2 Average differential energy spectrum of equivalent iron-like flux capable of leaving etchable tracks in lunar material [see text and Eq. (1b)].

In addition to the dominant iron tracks there occasionally occur longer tracks resulting from heavier cosmic rays. Price et al., (1971) have reported such tracks, including two tracks most likely from lead- or uranium-like nuclei. Such long tracks may allow us to study the ancient relative abundances of extremely heavy cosmic ray nuclei, provided we can determine the depth history of the rock (the heavier nuclei are more strongly attenuated with depth).

COSMIC RAY AND SPALLATION TRACKS

In order to understand what the cosmic ray and spallation track record can tell us about lunar surface history, we first must know the depth dependence of the production rate of these tracks. For the cosmic ray tracks we need the average energy spectrum of the heavy cosmic ray nuclei, predominantly the iron group, shown in Fig. 2. The spectrum is composed of two parts: a lower-energy solar contribution resulting from solar flare activity, and a galactic contribution at higher energies.

The relative nuclear abundances and shape of the galactic spectrum have been measured in satellite and balloon experiments (Comstock et al., 1969; Freier and Waddington, 1968; Price et al., 1968, 1970a; Munoz and Simpson, 1969) during times of minimum solar activity. We have corrected this shape for the average effect of solar modulation over the 11-year solar cycle using a model by Wang (1970). The contribution of each species to the production of etchable tracks is proportional, among other things, to the etchable track length $\Delta R(Z)$ and the relative abundance $A(Z)$. The abundance $A(Z) \approx 0$ for species with $Z > 26$ and $\Delta R(Z) = 0$ for $Z < 20$ to 23 for lunar material (Bhandari et al., 1971b; Plieninger and Krätschmer, 1971). Measured $A(Z)$ and plausible values of $\Delta R(Z)$ are listed in Table II.

Table II

Measured A(Z) and Plausible Values of ΔR(Z)

Species	Z	A(Z)*	ΔR(Z)**
-	< 23	-	0
vanadium	23	0.20	2.5 μm
chromium	24	0.55	5.5
manganese	25	0.44	8.5
iron	26	1.00	11.5
-	> 26	≈ 0	-

* Average of Price et al. (1968b, 1970a) and Munoz and Simpson (1969).

** Bhandari et al. (1971b) (but see Plieninger and Krätschmer, 1971, and Rajan and Price, 1971, who report larger values of ΔR(Z).)

The other factors which contribute to the track production rate [see Eq. (2)] have much weaker charge dependences over the dominant charge interval. Hence we may define an equivalent iron-like flux given by

$$\left(\frac{dN}{dT}\right)_E = \left(\frac{dN}{dT}\right)_{Fe} \sum_{\text{all } Z} \left(\frac{\Delta R(Z)}{\Delta R(Fe)}\right)\left(\frac{A(Z)}{A(Fe)}\right) \qquad (1a)$$

where (dN/dT) is the differential particle flux. The values listed in Table II yield

$$\left(\frac{dN}{dT}\right)_E = 1.63\left(\frac{dN}{dT}\right)_{Fe} = 0.52\left(\frac{dN}{dT}\right)_{VH}. \qquad (1b)$$

Equation (1b) gives the equivalent flux, corrected for average solar modulation, which is plotted for the galactic contribution in Fig. 2. This flux is about a factor of two less than that given by Fleischer et al. (1967) and Crozaz et al. (1970), which is the total flux of the larger VH charge group ($Z \geq 20$) treated as entirely iron, so that

$$\left(\frac{dN}{dT}\right)_E = \left(\frac{dN}{dT}\right)_{VH}. \qquad (1c)$$

Note that the lower flux of Eq. (1b) will imply correspondingly greater galactic cosmic ray exposure times than values based on the higher flux of Eq. (1c). Plieninger and Krätschmer (1971) report that the registration threshold may in fact be as low as Z = 20 (Ca), in which case the equivalent flux $(dN/dT)_E$ will be greater than that given by Eq. (1b). However, the contribution from the species Ca-V will be small because of their lower values of A(Z) and ΔR(Z).

For the solar contribution we rely on the energy spectrum derived from cosmic ray tracks observed in a piece of Surveyor III filter glass (Barber et al., 1971a; Crozaz et al., 1971; Fleischer et al., 1971b). The registration threshold for this glass is somewhat lower than for lunar minerals; however, the relative abundances of solar flare species P-Mn is so low that the charge interval effectively recorded by the Surveyor III glass is essentially the same as that recorded by lunar material (Fleischer et al., 1971b). The major uncertainty in applying the Surveyor III flux to lunar material is that the Surveyor III spacecraft was on the moon for only a fraction of the present solar cycle, about 2.6 years, during the period of maximum solar activity. It is not certain how the Surveyor III flux relates to the average solar contribution over many solar cycles. If the present cycle is typical, then the average solar flux should be about half of the observed Surveyor III flux, as plotted in Fig. 2.

From this composite energy spectrum we calculate the production rate of cosmic ray tracks in lunar material, given by

$$\dot{\rho}(\vec{r}) = \alpha \int_{\Omega} \left(\frac{dN}{dT}\right) E \left(\frac{dT}{dR}\right)_{Fe} \Delta R(Fe)\, e^{-\chi(\theta,\Phi)/\lambda}\, p(\theta,\Phi)\, d\Omega \qquad (2)$$

where α is the etching efficiency; $(dN/dT)_E$ is the equivalent iron-like flux defined earlier, evaluated at T which is the incident kinetic energy per nucleon corresponding to range $\chi(\theta,\Phi)$ in lunar rock or soil; $(dT/dR)_{Fe}$ is the rate of energy loss of iron in lunar minerals evaluated at T; λ is the mean particle loss path length due to nuclear interactions; $p(\theta,\Phi)$ is a projection function which takes into account the orientation of the etched surface with respect to rock or soil surface (Fleischer et al., 1967); and $\chi(\theta,\Phi)$ is the particle path length from the sample point to the surface in the direction of the solid angle increment dΩ. Since the original orientation of the etched surface is often unknown, we compute the average production rate for a set randomly oriented crystals for which case $p(\theta,\Phi) = 1/2$.

The cosmic ray track production in lunar soil derived in this way is shown in Fig. 3. It is clear from this curve that we expect a steep gradient in track density within a millimeter of the exposed surface. This steep production rate extends down to within ~1 μm of the surface as discussed at this conference by Borg et al. (1971b).

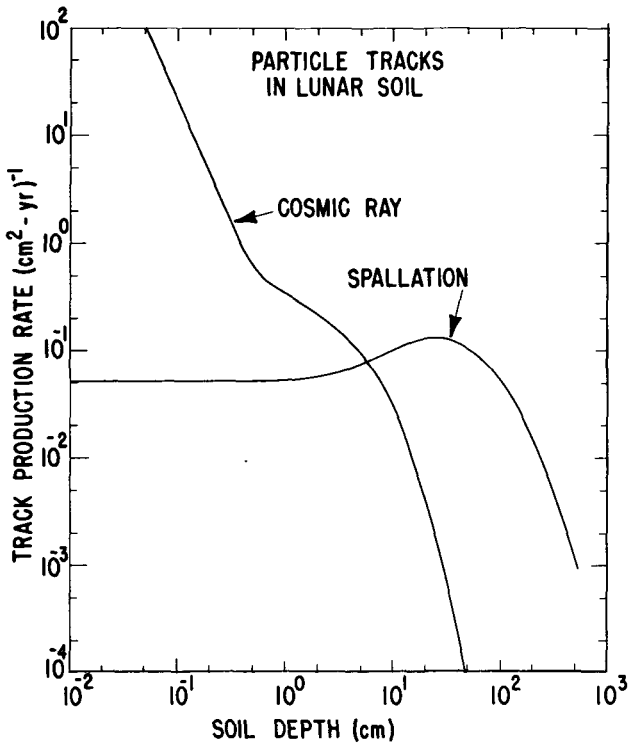

Fig. 3 Calculated rate of production of cosmic ray tracks [from Eq. (2) with ΔR(Fe) = 11.5 μm] and empirical production rate of spallation tracks, shown for semi-infinite lunar soil (density 1.6 g/cm³). These curves apply also to semi-infinite rock if the depth scale is decreased by a factor of about 2.

The second curve shown in Fig. 3 is the spallation track production rate determined from the high-energy cosmic ray proton flux and from laboratory production experiments (Kohman et al., 1967), including calibration of the response of individual lunar grains (Fleischer et al., 1971a--the magnitude of the production rate in individual grains was found to vary by ±70% from the average value indicated in Fig. 3). Because of the production of various secondary particles capable of inducing spallation reactions, the production of spallation recoil nuclei capable of leaving etchable tracks rises to a maximum at about 25 cm of soil.

We emphasize that these two production curves have very different shapes so that each yields different information about the history of a sample. Spallation tracks record the time spent in about the upper 2 meters of soil. Most of the cosmic ray tracks, on the other hand, were formed while the rocks or soil grains were situated on or within a few centimeters of the surface.

Table III

Fossil Track Ages (10^6 yrs) of Lunar Rocks

Sample Number	Cosmic Ray Surface Residence Times top/bottom (High age)*	(Low age)**	Spallation Recoil Tracks+ Surface Age	Minimum Age	Radiometric Spallation Ages‡
10017	11.2 total	5.7 total	420	170	200-640
10044	8.4 total	4.3 total	270	110	56-100
10049	57 total	29 total	21	8.5	22.5-25
12002	47/0	24/0	55	20	50-145
12017	1.4/2.0	0.7/1.0	105	40	-
12021	25/25	13/13	740	300	300
12065	27/0	14/0	170	70	160-200

* From Equ. 1b and $\Delta R(Fe) = 11.5$ μm.

** Fleischer et al. (1970c, 1971a) using Eq. 1c. Note that the Low age is also consistent with Eq. 1a and $\Delta R(Fe) \approx 20$ μm (Rajan and Price), so that the High and Low ages represent the limits of uncertainty in $\Delta R(Fe)$.

+ Fleischer et al. (1971a).

‡ Spread of values from various authors, see Fleischer et al. (1971a) for references.

LUNAR ROCKS AND EROSION RATES

We define for the rocks two spallation track residence times: the "surface age" determined by assuming that irradiation occurred entirely on the surface, and a "minimum age" which assumes that the irradiation occurred at the maximum rate. Typical track ages are given in Table III along with radiometric spallation ages determined by various workers.

A typical rock studied has a radius of a few centimeters, so that the cosmic ray track density at its center is due primarily to galactic cosmic rays. If the rock erosion rate is not too great, these central tracks may be used to find the "cosmic ray surface residence time" T_s by assuming

$$T_s = \rho(R) / \dot{\rho}(R) \qquad (3)$$

where $\rho(R)$ is the observed track density at the center of the rock and $\dot{\rho}(R)$ is calculated taking into account the shape and orientation of the rock. In Table III we have listed some values of T_s based on both Eq. (1b) (High age) and on Eq. (1c)(Low age).

The spallation and radiometric ages in Table III show the same trend from rock to rock. Most of these ages are greater than the cosmic ray surface residence times, indicating that the rocks have resided for some time below the surface but within the top 2 meters. For rocks 10049 and 12002 the spallation surface ages and radiometric ages are comparable to the cosmic ray surface residence times, indicating a simpler history. Rocks 12002 and 12065 have been irradiated on one side only.

Close to the surface of the rock, for a side which was facing up at some time, one finds a cosmic ray track gradient due to the solar flare particles (Fig. 4). A similar gradient on the opposite side indicates that the rock has had more than one orientation on the lunar surface. The observed gradient is generally less than the gradient predicted by Eq. (2) which has an exponent of about -2.4. This is generally regarded as an effect of rock erosion (Crozaz et al., 1970, 1971; Fleischer et al., 1971b; Barber et al., 1970b, 1971a, b.)

In Fig. 4 the solid curves refer to a vertical cross section through a spherical rock of final radius 3 cm which has resided in one orientation on the

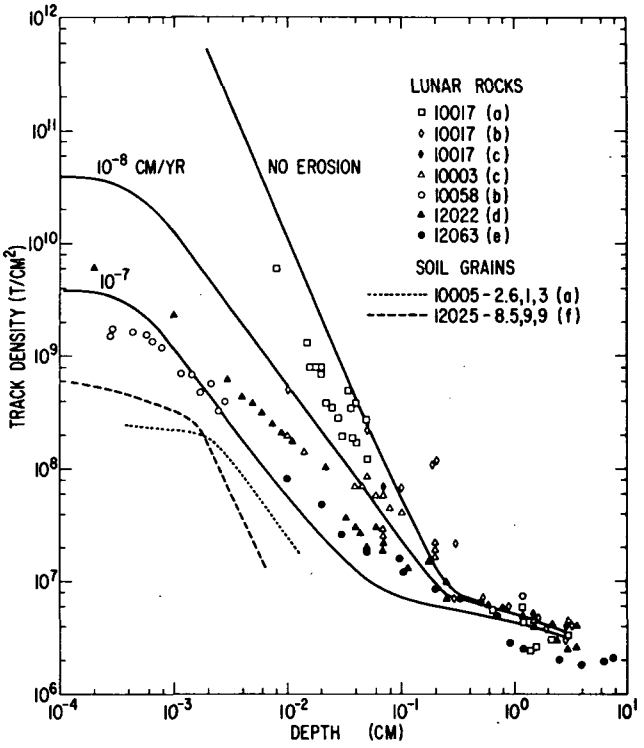

Fig. 4 Cosmic ray track gradients observed in several lunar rocks and two soil grains. The solid curves are calculated for a typical rock undergoing no erosion, and for two finite erosion rates. (a) Fleischer et al. (1970c); (b) Crozaz et al; (c) Price and O'Sullivan (1970b); (d) Barber et al. (1971a); (e) Crozaz et al. (1971); (f) Fleischer et al. (1971a) and Fig. 5.

surface for T_S = 15 m.y. The no-erosion curve is derived from Eqs. (1b), (2), and (4):

$$\rho(d) = \dot{\rho}(d)\, T_S. \qquad (4)$$

The curves for finite erosion rates e = 10^{-8} cm/yr and 10^{-7} cm/yr are derived from Eqs. (1b), (2) with a time-dependent radius r = R + e(T_S - t) and

$$\rho(d, e) = \int_0^{T_S} \dot{\rho}(d, et)\, dt = \frac{1}{e} \int_R^{R+eT_S} \dot{\rho}(d, r)\, dr, \qquad (5)$$

where d is the final depth below the rock surface, e is the erosion rate, and R is the final radius.

These curves are not meant to fit any particular rock. For ρ near the center of a given rock we must take into account its shape and size, the time it has spent in each orientation on the lunar surface, and the possible contribution from irradiation before direct surface exposure. For example, rock 12063 has spent less time on the surface than the others. Below about 1 mm, however, the track density is essentially independent of the size and shape of the rock. Still closer to the surface the track density in an eroding rock becomes independent of the surface residence time as well, as the production rate comes into equilibrium with the eroding surface. More precisely, as the surface residence time T_S increases the track density at each depth approaches a maximum or equilibrium value given by

$$\rho_E(d, e) = \frac{1}{e} \int_R^{\infty} \dot{\rho}(d, r)\, dr. \qquad (6)$$

For surface residence times on the order of 10 m.y. the track densities derived from Eq. (5) coincide with the equilibrium values at depths less than a few hundred microns for erosion rates e ≤ 10^{-7} cm/yr. Greater depths (to d ~ e T_S) would also be in equilibrium if it were not for the effects of the galactic contribution and the finite size of the rock. Below a few hundred microns, therefore, the magnitude of the track density depends only on the erosion rate and the average flux of solar flare particles [Eq. (6)]. The slope of the track gradient in this near-surface region depends on the exponent of the solar flare energy spectrum but may be modified by irregular erosion or chipping, unevenness of the surface near the sample point, and possible loss of surface material during transport from the moon. For example, if rock 10058 has lost ~10μ (one layer of unusually small grains) during transport, then it should be plotted coincident with rock 12022 in Fig. 4.

The data shown in Fig. 4 (see references in figure caption) indicate erosion rates varying from e < 10^{-8} cm/yr for 10017 to 3 x 10^{-8} cm/yr for 12022 and ~5 x 10^{-8} cm/yr for 12063. Crozaz et al. (1971) argue that the average solar particle flux may be a factor of two greater than we have used in deriving the curves in Fig. 4 and hence obtain proportionally higher erosion rates. The low value implied for 10017 may indicate that there have been wide fluctuations in the micrometeoroid flux at the moon's surface. 10017 may have spent most of its surface exposure time during a period of meager micrometeoroid activity, then was buried and brought to the surface again less than 0.3 m.y. ago (corresponding to <100μ of erosion at the rate of 3 x 10^{-8} cm/yr).

Unique opportunities to study solar flare activity in the past without the uncertainties of rock erosion are provided by rocks which have been recently covered with a glass coating; the best example of this is rock 12017 (Fleischer et al., 1971a). Although cosmic ray tracks in the center of the rock indicate that 12017 has been on the surface for at least 1.7 m.y., cosmic ray tracks found in grains imbedded within the glaze itself indicate that the glaze has been exposed on the rock for only 9000 years. These tracks show the decrease with depth

arising from solar flare particles. The glass coating is much less retentive of tracks than the mineral crystals; tracks in the glaze should fade away after about 500 years on the lunar surface due to thermal annealing (Fleischer et al., 1971a). The track density in the glaze also decreases with depth but has a lower magnitude than the track density in imbedded crystals, consistent with the ~500 year retention time and the present flux of solar flare particles.

LUNAR SOIL

The record of particle tracks in the individual soil grains indicates a history even more complex than that of the rocks. (Hereinafter, the phrase "track density" will refer to cosmic ray tracks, not spallation tracks, unless otherwise noted.) For the purposes of discussion we may divide the soil grain samples into three groups according to track density: 1. $\rho \geq 5 \times 10^8$ cm^{-2}, 2. ρ with a strong gradient, and 3. $\rho \lesssim 5 \times 10^8$ cm^{-2}.

1. Grains with high track densities include very many micron-sized grains and micron-deep coatings on larger grains (Borg et al., 1971a, b) containing 10^{10} to 10^{12} cm^{-2}. Very high densities have also been reported throughout some larger grains (~100μ radius) (Crozaz et al., 1971; Barber et al., 1971a, b). These track densities must be the result of direct exposure to space for $T_s \sim 10^4$ to 10^5 yr for the micron-sized grains and considerably longer for the larger grains.

2. The second class of samples includes grains of ~100 micron-radius which contain a steep track density gradient extending inward from one or two edges. These have track densities typically approaching $\rho \sim 10^9$ cm^{-2} in the outer 10μ, dropping to $\rho \sim 2 \times 10^7$ cm^{-2} in the center or low-density edge. A contour map of one such gradient is shown in Fig. 5. Contours such as this may be strongly affected by the shape of the grain, but in general they are what one expects if the grain had been exposed on the lunar surface in a particular orientation and covered by no more than several microns of dust.

Track density profiles measured at 7500X along the steepest track gradients of two such grains are shown in Fig. 4. There are two possible conditions under which tracks may have been accumulated to produce such gradients: (a) the grains were tossed randomly to the very surface as part of an ejecta blanket and later buried, or (b) the tracks accumulated while the grains were still part of an eroding rock, eventually being exposed, chipped out, and buried in the soil.

Consider first case (a). The dominant erosion processes are discrete events, well separated in time, which will tend to destroy or bury a soil grain. Hence while the grain is on the surface (case a) the acquired track gradient should follow a no-erosion curve given by Eq. (4) for some surface residence time T_s. In this case we interpret the sharp breaks

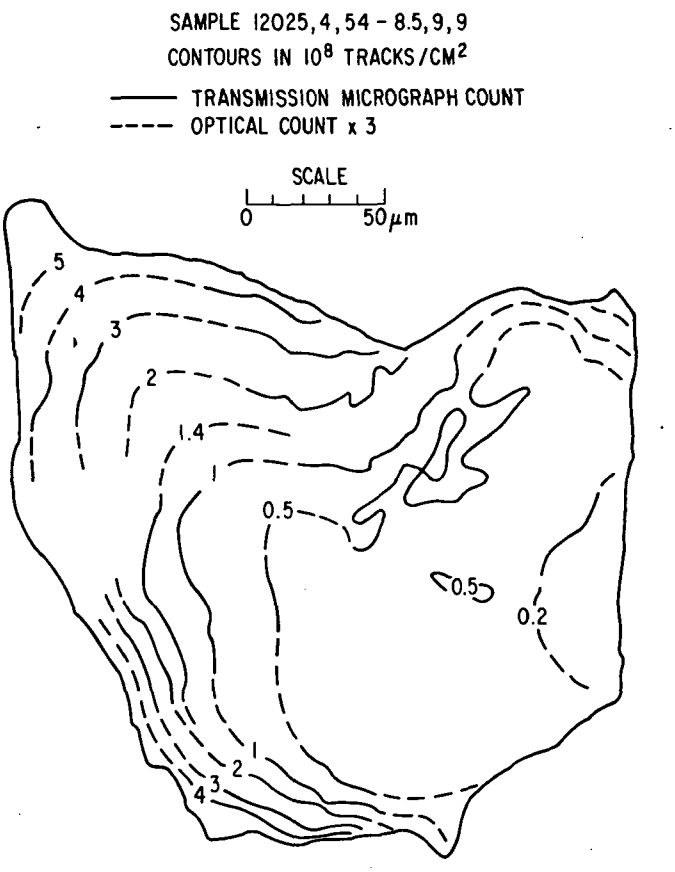

Fig. 5 Contour map of cosmic ray track density in a pyroxene soil grain with strong track gradient. The grain was found 8.5 cm below the lunar surface.

in these curves at ≈20μ as being due to an (uncorrected-for) shielding of several microns of dust, which is reasonable considering the cohesiveness of the soil. For the soil grains plotted in Fig. 4 we infer $T_s \sim 10^4$ yr, which is consistent with the rate of disturbance of a surface grain by micrometeoroid bombardment (Shoemaker et al., 1970).

If case (a) is the predominant condition for soil-grain gradient production, then we should expect a wide range of track densities from grain to grain corresponding to an exponential distribution in surface residence times. This in turn would yield information on the rate of disturbance of the surface.

In case (b) the track gradient in the grain represents the gradient which existed in the upper ~100μ of the parent rock at the time when the grain was chipped out. (The grain could not have come from the interior of the rock since in that case the observed gradient would be too steep.) Hence the track gradients for the soil grains in Fig. 4 should be fitted by equilibrium curves satisfying Eq. (6) for whatever erosion rates were experienced by the parent rocks. The implied erosion rate is $\approx 3 \times 10^{-7}$ cm/yr for

both grains shown, or about an order of magnitude greater than the average rate observed in the rocks presently on the surface. This higher rate presumably would be related to the greater rate of meteoroid bombardment early in the moon's history which would imply an early epoch for the formation of these soil grains from their parent rocks. If case (b) is the predominant condition for soil-grain gradient production, then we should expect a relatively narrow range of track densities from grain to grain (~ factor of 10) corresponding to the distribution of erosion rates experienced during the period of soil formation. Rock 10017 indicates that the erosion rate may vary considerably, but most of the soil gradients originating in rocks will be produced during times of higher erosion rates.

Both conditions (a) and (b) should occur; we have indicated how the dominant condition can be determined from the statistical distribution of track densities in grains with track gradients. In principle we could distinguish between conditions (a) and (b) by appealing to the slopes of the track gradients (Fig. 4). In practice these slopes are strongly affected by the shape of the grain, by uneven shielding during irradiation, and by loss of material by soil abrasion. Careful mapping of many grains, however, may yield a meaningful average slope. In the above discussion we have assumed that the average level of the solar flare particle flux is the same now as it was when the track gradients were recorded. There is no reason to suppose that this is not true. However, long-range variation in flare activity remains a possible, though less likely alternative to variation in erosion rate.

3. The third broad class of soil grains consists of those which have a uniform track density $\rho < 5 \times 10^8$ cm^{-2}. The lack of a track gradient or very high track density indicates that these grains have never been within a few hundred microns of the surface. Their cosmic ray track record is the result of exposure within the top ~10 cm of soil (Fig. 3) and hence is determined by the history of soil activity.

In the discussion of soil activity which follows we combine the third class of grains with the track densities measured in the center of soil grains having track gradients (the latter being about 20% of the combined population). These two groups have similar frequency distributions for both cosmic ray and spallation track densities (Comstock et al., 1971) and hence have a similar subsurface history.

In Fig. 6 we have indicated the distribution of cosmic ray track densities in individual soil grains with $\rho < 5 \times 10^8$ cm^{-2} for several depths in the Apollo 12 double core (Comstock et al., 1971). Bhandari et al., (1971a) have measured similar distributions at additional depths. The data points give the median track density observed at each depth and the limit bars show the spread of the 70% of the samples closest to the median. The statistical error

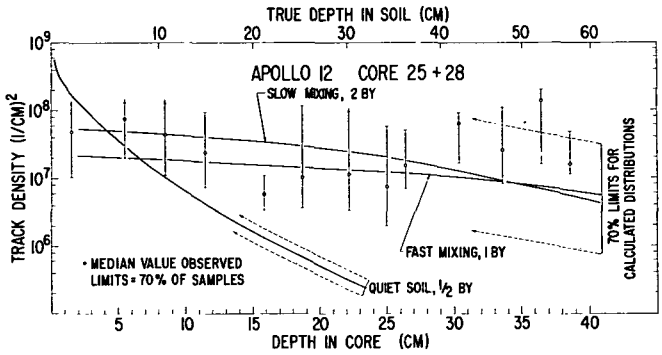

Fig. 6 Cosmic ray track distribution in double-core 12025+28. The data points indicate the observed spread in track density from grain to grain. The curves have been calculated for some models of soil history discussed in the text (see Comstock et al., 1971, for a complete discussion of the data and calculations). The true soil depths are given by Carrier et al. (1971).

in the measurement of these track densities is typically $\lesssim 10\%$, so the wide spread in track densities is due to a complex irradiation history for each depth. The "Quiet soil" curve (Fig. 6) is calculated from Eqs. (2) and (4) for an irradiation time of 500 m.y. Clearly this curve is not consistent with the observations--considerable soil movement has taken place.

As one approximation to this movement we might assume that the soil has suffered continual depth-dependent mixing by meteoroid impact (Shoemaker et al., 1970). We have worked out computer models based on this assumption (Comstock et al., 1971), and the results of two such models are shown in Fig. 6 by the curves marked "slow mixing" and "fast mixing." Fast mixing refers to soil mixed to depths d_c in time periods τ(m.y.) = d_c (cm); slow mixing is ten times slower. The mixing time derived by Shoemaker et al. (1970) for soil is $\tau \approx 1.6\, d_c$ for $d_c \sim 10$ to 100 cm. The solid curves in Fig. 6 give the calculated median values with the 70% spread of hypothetical samples and irradiation times as indicated. It is seen that the magnitude and overall distribution of observed track densities are well reproduced by these models.

On the other hand, the track density distributions do appear to contain some structure, which is even more evident with the greater statistics given by Bhandari et al. (1971a). In addition the Apollo 12 double core has some well-defined visual layers, perhaps as many as 13, through the 60 cm depth of the sampled soil (LSPET, 1970). At least one of these layers correlates strikingly with the structure in the track distributions. This is the coarse layer at a true soil depth of ≈16 to 20 cm which contains a relatively low track density.

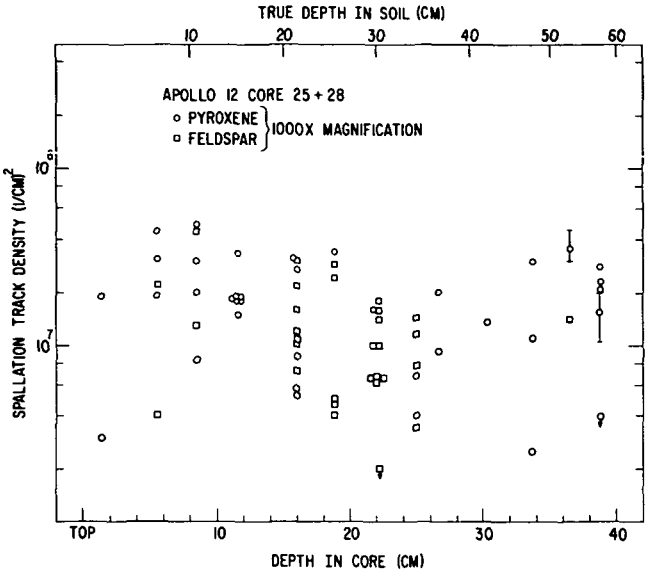

Fig. 7 Preliminary spallation track distribution in double-core 12025+28 (see Comstock et al., 1971, for a complete discussion of the data).

Another model which approximates the movement of the soil has been investigated by Bhandari et al. (1971a). They assume that the soil has been steadily buried by deposited layers, with no mixing between layers and no irradiation prior to deposition. From the track densities in each layer they derive surface residence times for each layer on the order of 0 to 60 m. y. Bhandari et al. find that some mixing must still be invoked within each layer in order to explain the distribution of track densities within that particular layer.

Spallation tracks can give us further information on the history of the soil grains. In Fig. 7 we have plotted a preliminary distribution of spallation track densities in the Apollo 12 double core. Here again we see a spread, although not as broad as for the cosmic ray tracks. As pointed out by Comstock et al. (1971), the pattern shown here would be expected on the basis of a soil mixing model; but a burial model with no previous irradiation would predict a spallation track density that continued to increase with depth by a factor of ~10 in the top 60 cm, due to the high spallation production rate (Fig. 3). The spallation tracks in Fig. 7 force us to conclude that most of the grains have been pre-irradiated in the top 2 meters of soil, or 1 meter of rock, for an integrated time of ~100 m. y. before excavation, deposition, and burial at the core site. This implies a more complex history than simple burial after a single excavation from virgin (trackless) material, for most of the layers.

We know that the moon is continually bombarded by meteoroids, so that some depth-dependent mixing must be taking place (Opik, 1969). The nature of these events is such that material is removed from an excavation and deposited in a thin layer around the site. At a given point on the moon this layering will continue to build up the soil level until an impact occurs near that point, re-excavating some of the deposited material. We know further that there is a correlation between deposition distance from the excavation site and original stratigraphy at the excavation site (Schmitt and Sutton, 1971). The layer deposited at a given point comes from a rather restricted depth interval and thus represents a mixing of only a few of the original layers. Hence each layer may have a distinctly different history. At a given site some layers will have been excavated from deep, previously unirradiated material, while others will be composed of a more mature, better mixed population of soil.

The question which we ask is: What can we say about the mixing history of each observed layer? Our approach to this question appeals again to the mixing model calculations. These calculations (Comstock et al., 1971) describe material which has been exposed for some time at various depths in the upper 25 cm of soil, mixed occasionally with nearly trackless material exposed only at greater depths. As a first approximation this should be similar to the mixing of layers with different exposure histories. Comstock et al. (1971) assumed that the entire double core sample represents one homogeneously mixed population. We now assume that the previous history of a given layer (i. e., before deposition and burial at its present site) is reproduced by a mixing model for some mixing age appropriate to that particular layer.

A layer which is composed of what we shall refer to as "well-mixed" material should have a track density distribution similar to that shown in Fig. 8. This distribution is the result of Monte Carlo calculations for hypothetical soil grains subjected to depth-dependent mixing and irradiation for 2800 m. y. It is seen that most of the samples are included in an order-of-magnitude spread around $\rho \approx 10^8$ cm^{-2} and many samples occur with $\rho \gg 10^8$ cm^{-2}. A track density distribution calculated for a soil population which has been mixed for only 1200 m. y. is shown in Fig. 9. Here we have a broader distribution with $\rho \sim 10^6$ to 10^8 cm^{-2} but still including some samples with $\rho \gg 10^8$ cm^{-2}. A sample grain population of this kind we shall refer to as "partially mixed."

Soil which has been recently excavated from previously undisturbed material will have $\rho \ll 10^6$ cm^{-2} (Fig. 3). Whatever cosmic ray tracks these grains have were formed after the layer was deposited on the surface. These layers will have predominantly low track densities $\rho \sim 10^6$ to 10^7 cm^{-2} with very few, if any samples with $\rho \gtrsim 10^8$ cm^{-2}. We will refer to such layers as "unmixed" although it is understood that some very shallow mixing within the layer must take place during its surface residence time.

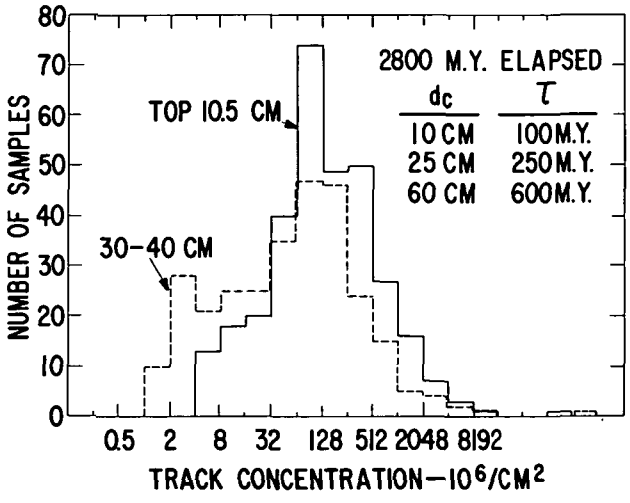

Fig. 8 Calculated distributions of cosmic ray track density after 2.8 b. y. of soil mixing and irradiation. Hypothetical samples were periodically mixed down to three characteristic depths dc with time periods τ. These distributions are characteristic of well-mixed soil.

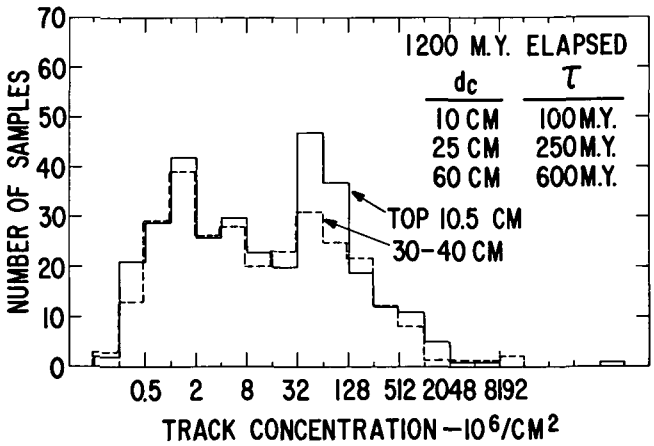

Fig. 9 Calculated distributions of cosmic ray track density after 1.2 b. y. of soil mixing and irradiation. These distributions are characteristic of partially mixed soil.

By using Figs. 8 and 9 as prototypes we compare these definitions with the track density distributions found in the various physical layers observed in the Apollo 12 double core (LSPET, 1970). From Fig. 6 and the detailed distributions given by Bhandari et al. (1971a) we identify a mixing history with each physical layer in Table IV. The low track density reported for layer VI identifies it as material from an unmixed population. (The samples at ≈20 cm in Fig. 6 may be associated with this.) For layers II, III-1, VII, VIII, and X the track density distributions

Table IV

Mixing History of Physical Layers

Layer Designation*	Maximum Soil Depth**	Mixing History
X	1.6 cm	well mixed
IX	3.1	partially mixed
VIII	11.8	well mixed
VII	16.1	well mixed
VI	19.6	unmixed
V	24.0	well mixed
IV	29.7	partially mixed
III-4	35.2	well mixed
III-3	38.8	well mixed
III-2	43.2	partially mixed
III-1	52.2	well mixed
II	58.8	well mixed
I	≥60.5	partially mixed

* LSPET (1970); Bhandari et al. (1971a).

** Carrier et al. (1971); LSPET (1970).

given by Bhandari et al. (1971a) show sharp peaks in the interval $\rho \sim 3 \times 10^7$ to 10^8 cm^{-2} corresponding to the derived distribution for well-mixed soil (Fig. 8). The track distributions for layers I and IV are much broader, similar to the distribution in Fig. 9 calculated for partially mixed soil. The other layers, III-2, III-3, III-4, V, and IX, appear to be intermediate between Figs. 8 and 9.

When compared with physical features (LSPET, 1970) we find that those layers identified as well mixed tend to be medium grey, with no internal structure, generally finer grained with unclear boundaries. This is consistent with a longer history of physical activity (excavation, deposition, abrasion) and a greater homogeneity. The layers identified as partially mixed generally have discernible boundaries and some differences in physical properties. The unmixed layer VI is easily distinguishable from the others and is coarser grained, consistent with recent excavation from "virgin" material.

In general, the better-mixed soil has been subjected to more physical activity and more admixture from different localities and depths, tending to be more homogeneous with more of the grains well irradiated by cosmic rays.

The identification of mixing histories allows us to make another inference about the physical layers. In Fig. 10 we have plotted the distribution of approximate thicknesses of the visual layers, corrected for compaction (Carrier et al., 1971). In addition we have drawn a curve $P(\ell) \sim 1/\ell^2$ representing the expected distribution of thicknesses. This curve was

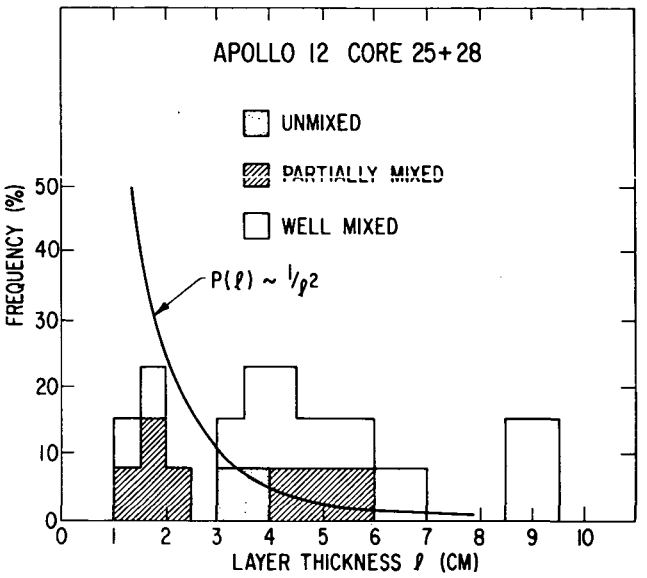

Fig. 10 Frequency distribution of true soil thicknesses of the visual layers in double-core 12025+28. Assigned mixing histories are indicated (Table IV). The curve P(ℓ) represents an expected frequency distribution.

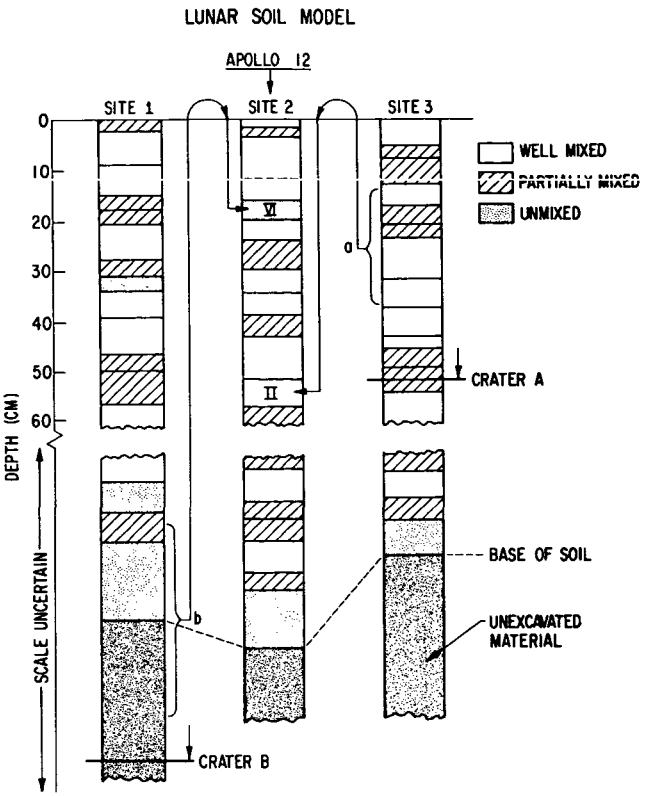

Fig. 11 Hypothetical lunar soil illustrating the formation of Apollo 12 double-core layers II and VI according to a model described in the text. Arrangement of the hypothetical parent layers at sites 1 and 3 is not unique.

derived by assuming that excavated material is deposited outside the crater in a smoothly thinning blanket (Opik, 1969) within 1 to 2 diameters of a crater site and taking into account the size-frequency distribution of cratering events (Shoemaker et al., 1970). Figure 10 suggests an overabundance of thick layers. However, the thickest layers have been identified as well mixed; hence they may have been built up from several smaller layers of well-mixed material which are not distinguishable because they are too homogeneous.

Our picture of lunar soil, based on the distribution of cosmic ray particle tracks, may be summarized by reference to Fig. 11 which shows the hypothetical formation of two of the Apollo 12 double-core layers. Figure 11 shows three hypothetical sites; the upper part of site 2 is drawn to represent the Apollo 12 double core 25 + 28. The three sites are shown at three different times, site 3 at an early time T_1, site 1 at a later time T_2, and site 2 at the present. Each site has been built up by repeated layering (presumably of ejecta blankets). Specifically, we suppose that at time T_1 an impact occurred at site 3 excavating material down to some depth such as that marked "Crater A." Excavated material from some depth interval (marked a in Fig. 11) was deposited on the surface at site 2 and has become what we know as layer II. Since this material was already fairly well mixed at site 3 it forms a well-mixed layer at site 2. If the original layers in depth interval a at site 3 had been predominantly partially mixed, or included an unmixed layer, then the material deposited at site 2 would have been only partially mixed. Between times T_1 and T_2 other layers were deposited at site 2 on top of layer II. Note that the final layering sequence was not necessarily deposited contiguously, that is, several layers may have been deposited on top of layer II, then some of these re-excavated by shallow cratering events and replaced by other layers.

At the later time T_2 we suppose that an impact event occurred at site 1, excavating material to a great depth (crater B in Fig. 11). Unirradiated soil or subsoil material (depth interval b in Fig. 11) was deposited on the surface at site 2, forming the coarse layer VI. Further layering and possibly shallow excavations occurred at site 2 between time T_2 and the present when the observed layer sequence was sampled.

We have shown that most of the observed layers may come from partially or well-mixed material, so that most soil grains have experienced several excavations and surface exposures. Each particular surface residence time may therefore be much less than the integrated surface residence time. Since most of the cosmic ray tracks are acquired near the

surface, the surface residence times derived by the method of Bhandari et al. (1971a) for the individual layers will be similar to average integrated surface residence times for the soil grains in those layers.

The existence of layers is not inconsistent with mixing by excavation because the stratigraphy below a given depth is not destroyed by excavation of material above that depth. Frequent excavation above a depth d means that the net burial rate at depth d in general will be less than the average layering rate on the surface. It is expected that spallation tracks in the soil, with their high rate of production in the upper 2 meters, can provide information about this net burial rate, especially for layers with a simple cosmic ray irradiation history (e. g., Apollo 12 double-core layer VI).

A relevant physical process which has not been discussed above is the possibility of surface transport (e. g., Gold, 1971). Surface transport over great distances will require that soil grains remain on the surface for relatively long times and can be expected to acquire quite high cosmic ray track densities (the center of a 100-μm-diameter grain on the soil surface will acquire cosmic ray tracks at a rate of $\dot{\rho} \sim 10^3$ cm^{-2} -yr). Such transport probably can be ruled out for the grains in layer VI (Table IV) which have $\rho \sim 10^7$ cm^{-2} (Bhandari et al., 1971a). On the other hand, large grains which have very high track densities, $\rho > 10^9$ cm^{-2} (Barber et al., 1971a, b; Crozaz et al., 1971), represent prolonged exposure and the possibility of surface transport for these grains cannot be eliminated.

CONCLUSIONS

The particle track record of lunar surface history for both rocks and soil can be summarized in three general depth domains (Fig. 3).

1. Direct surface irradiation by solar flare heavy nuclei of the first 0 to ~0.2 cm results in steep track density gradients which have recorded rock erosion rates of about 10^{-8} to 10^{-7} cm/yr (Fig. 4). Track gradients in soil grains may indicate a parent rock erosion rate of $\sim 3 \times 10^{-7}$ cm/yr early in the moon's history. When the exposure time and erosion rate are known, such as for the glass coating on 12017, then the level of solar particle flux in the past can be determined.

2. The second depth domain, ~0.2 to ~10 cm, involves irradiation primarily by galactic cosmic ray heavy nuclei. These particle tracks have provided surface residence times for the rocks of ~1 to 50 m. y. (Table III). Cosmic ray tracks (Fig. 6) acquired predominantly at these depths record the mixing and layering history of lunar soil. Track distributions in the soil are consistent with a soil history which includes repeated excavation, layering, and burial, such that one-core 12025+28 soil layer is unmixed and weakly irradiated, whereas the others contain soil which has been better and better mixed while being more and more irradiated (Table IV).

3. The third depth domain, 0 to ~200 cm, is recorded by the tracks of spallation-recoil nuclei. These tracks indicate that both the rocks and soil grains have a wide range of residence times in the top 2 meters of the lunar surface (Table III, Fig. 7).

ACKNOWLEDGMENTS

The author is indebted to R. L. Fleischer and H. R. Hart, Jr. for many helpful comments.

REFERENCES

Barber, D. J., Cowsik, R., Hutcheon, I. D., Price, P. B. and Rajan, R. S., Proc. Second Lunar Science Conf., Houston, Texas (1971a) (in press).

Barber, D. J., Hutcheon, I. D. and Price, P. B., Science, 171, 372 (1971b).

Bhandari, N., Bhat, S., Lal, D., Rajagopalan, G., Tamhane, A. S., Venkatavaradan, V. S., Arrhenius, G., Liang, S., Macdougall, D. and Wilkening, L., Proc. Second Lunar Science Conf., Houston, Texas (1971a) (in press).

Bhandari, N., Bhat, S., Lal, D., Rajagopalan, G., Tamhane, A. S., and Venkatavaradan, V. S., Proc. Second Lunar Science Conf., Houston, Texas (1971b) (in press).

Borg, J., Durrieu, L., Dran, J. C., Jouret, C. and Maurette, M., Proc. Second Lunar Science Conf., Houston, Texas (1971a) (in press).

Borg, J., Durrieu, L., Dran, J. C. and Maurette, M., Proc. I. A. U. Symposium No. 47, Newcastle upon Tyne, England, (1971b) (to be published).

Burnett, D., Monnin, M., Seitz, M., Walker, R. and Yuhas, D., Proc. Second Lunar Science Conf., Houston, Texas (1971) (in press).

Carrier, W. D., III, Johnson, S. W., Werner, R. A. and Schmidt, R. Proc. Second Lunar Science Conf., Houston, Texas (1971) (in press).

Comstock, G. M., Fan, C. Y. and Simpson, J. A., Astrophys. J., 155, 609 (1969).

Comstock, G. M., Evwaraye, A. O., Fleischer, R. L., and Hart, H. R., Jr., Proc. Second Lunar Science Conf., Houston, Texas (1971) (in press).

Crozaz, G., Haack, U., Hair, M., Maurette, M., Walker, R. and Woolum, D., Geochim. Cosmochim. Acta. Suppl. 1, 3, 2051 (1970).

Crozaz, G., Walker, R. and Woolum, D., Proc. Second Lunar Science Conf., Houston, Texas (1971) (in press).

Fleischer, R. L., Price, P. B., Walker, R. M., Maurette, M. and Morgan, G., J. Geophys. Res. 72, 355 (1967).

Fleischer, R. L., Hart, H. R., Jr., Jacobs, I. S., Price, P. B., Schwarz, W. M. and Woods, R. T., J. Applied Phys., 41, 958 (1970a).

Fleischer, R. L., Haines, E. L., Hanneman, R. E., Hart, H. R., Jr., Kasper, J. S., Lifshin, E., Woods, R. T. and Price, P. B., Science, 167, 568 (1970b).

Fleischer, R. L., Haines, E. L., Hart, H. R., Jr., Woods, R. T. and Comstock, G. M., Geochim. Cosmochim. Acta, Suppl. 1, 3, 2103 (1970c).

Fleischer, R. L. and Hart, H. R., Jr., Proc. Burg Wartenstein Conf. on Calibration of Hominoid Evolution, July 1971, and General Electric Research and Development Center Report No. 70-C-328 (1970d).

Fleischer, R. L., Hart, H. R., Jr., Comstock, G. M. and Evwaraye, A. O., Proc. Second Lunar Science Conf., Houston, Texas (1971a) (in press).

Fleischer, R. L., Hart, H. R., Jr. and Comstock, G. M., Science, 171, 1240 (1971b).

Freier, P. S. and Waddington, C. J., Phys. Rev., 175, 1641 (1968).

Gold, T., I. A. U. Symposium No. 47, Newcastle upon Tyne, England (1971).

Kohman, T. D. and Bender, M. L., in High Energy Nuclear Reactions in Astrophysics, B. S. P. Shen, Ed., pp. 169-245 (Benjamin, Inc., 1967).

Lal, D., Macdougall, D., Wilkening, L. and Arrhenius, G., Geochim. Cosmochim. Acta, Suppl. 1, 3, 2103 (1970).

LSPET (Lunar Sample Preliminary Examination Team), Science, 167, 1325 (1970).

Munoz, M. G. and Simpson, J. A., 11th Internat. Conf. on Cosmic Rays, OG-67, Budapest (1969).

Öpik, Ernst J., in Annual Review of Astronomy and Astrophysics, 7, pp. 473-526 (Annual Reviews, Inc., Palo Alto, Calif.).

Plieninger, T. and Krätschmer, W., (Abstract) Trans. Amer. Geophys. Union, 52, 268 (1971).

Price, P. B., Fleischer, R. L., Peterson, D. D., O'Ceallaigh, C., O'Sullivan, D. and Thompson, A., Phys. Rev., 164, 1618 (1967).

Price, P. B., Fleischer, R. L. and Moak, C. D., Phys. Rev., 167, 277 (1968a).

Price, P. B., Peterson, D. D., Fleischer, R. L., O'Ceallaigh, C., O'Sullivan, D. and Thompson, A., Phys. Rev. Lett., 21, 630 (1968b).

Price, P. B., Peterson, D. D., Fleischer, R. L., O'Ceallaigh, C., O'Sullivan, D. and Thompson, A., Hung. Phys. Acta, 29, Suppl. 1, 417 (1970a).

Price, P. B. and O'Sullivan, D., Geochim. Cosmochim. Acta, Suppl. 1, 3, 2351 (1970b).

Price, P. B., Rajan, R. S., and Shirk, E. K., Proc. Second Lunar Science Conf., Houston, Tex. (1971) in press.

Rajan, R. S. and Price, P. B. (to be published, 1971).

Schmitt, H. H. and Sutton, R. L., Proc. Second Lunar Science Conf., Houston, Texas (1971) (in press).

Shoemaker, E. M., Hait, M. H., Swann, G. A., Schleicher, D. L., Schaber, G. G., Sutton, R. L., Dahlem, D. H., Goddard, E. N. and Waters, A. C., Geochim. Cosmochim. Acta, Suppl. 1, 3, 2399 (1970).

Wang, J. R., Astrophys. J., 160, 261 (1970).

APPENDIX VII

Journal of Geophysical Research (submitted)

GENERAL ELECTRIC

GENERAL ELECTRIC COMPANY
CORPORATE RESEARCH AND DEVELOPMENT
Schenectady, N.Y.

DATING OF MECHANICAL EVENTS BY DEFORMATION-INDUCED ERASURE OF PARTICLE TRACKS

by

R. L. Fleischer, G. M. Comstock, and H. R. Hart, Jr.
General Physics Laboratory

Report No. 72CRD010 December 1971

TECHNICAL INFORMATION SERIES

CLASS 1

GENERAL ELECTRIC

General Electric Company
Corporate Research and Development
Schenectady, New York

TECHNICAL INFORMATION SERIES

AUTHOR	SUBJECT	NO.
Fleischer, RL Comstock, GM Hart, HR, Jr	particle tracks	72CRD010
		DATE: December 1971
TITLE: Dating of Mechanical Events by Deformation-Induced Erasure of Particle Tracks		GE CLASS: 1
		NO. PAGES: 3
ORIGINATING COMPONENT: General Physics Laboratory		CORPORATE RESEARCH AND DEVELOPMENT SCHENECTADY, N.Y.

SUMMARY

Natural, fine-scale, plastic deformation of a lunar pyroxene has been observed to fragment pre-existing charged particle tracks. An observer who is using only an optical microscope would have seen only the tracks formed after the deformation and hence would measure the time when deformation occurred, in this particular case an estimated 20 to 25 m.y. ago.

KEY WORDS

particle tracks, lunar materials, fission tracks dating, mechanical properties

INFORMATION PREPARED FOR _____

Additional Hard Copies Available From

Corporate Research & Development Distribution
P.O. Box 43 Bldg. 5, Schenectady, N.Y., 12301

Microfiche Copies Available From

Technical Information Exchange
P.O. Box 43 Bldg. 5, Schenectady, N.Y., 12301

DATING OF MECHANICAL EVENTS BY DEFORMATION-INDUCED ERASURE OF PARTICLE TRACKS*

R. L. Fleischer, G. M. Comstock, and H. R. Hart, Jr.

Particle tracks in solids are tools for dating natural events. The most usual time intervals that can be measured are solidification ages, which are determined by counting tracks from spontaneous fission (Price and Walker, 1963; Fleischer and Price, 1964 a, b; Fleischer and Hart, 1971). In addition, surface residence ages on atmosphereless bodies such as the moon can be measured by counting cosmic ray tracks (Crozaz et al., 1970; Fleischer et al., 1970). In each case the assumption is normally made that once tracks are formed they remain intact during subsequent time.

If this assumption of track permanence is in error, the most usual reason is thermally induced fading, which if undetected would lead to the calculation of an age that is less than the true solidification age (Fleischer and Price, 1964c). Happily, once it is realized that heating diminishes the diameters of etched tracks (Berzina et al., 1966) the effects of heating can be detected and appropriate corrections made (Storzer and Wagner, 1969).

Another environmental factor that can alter track permanence is deformation. In particular, the effectiveness of shock deformation in erasing tracks has been demonstrated in laboratory experiments (Fleischer et al., 1967; Ahrens et al., 1970) and in nuclear detonations (Fleischer et al., 1972). In neither of these cases, however, was it possible to establish a mechanism for track erasure.

One track erasure mechanism that has been proposed (Fleischer et al., 1965, 1969) is simply the subdividing of tracks by intersecting slip during plastic deformation. In the simplest case an intersecting slip line might bisect a track of length L and convert it into two tracks each of length L/2. In a more extreme case n cuttings of the track would convert it to n+1 pieces of average length L/(n+1), thereby dispersing the radiation damage. If the resulting track segments are too short to resolve in the microscope being used, the observer would conclude that no tracks are present and that the sample age is zero. If the tracks are observable but short, their length distribution is a measure of the scale of the deformation and their number measures the time from the start of track formation and storage to the time of deformation. The number of unshortened tracks formed after deformation measures the time since the deformation event.

Here we wish to report what we believe is the first identification of the natural fragmentation and effective erasure of tracks by plastic deformation. Figure 1 shows examples of etched tracks in two lunar pyroxenes from the Apollo 12 mission. The tracks have been replicated using cellulose acetate which was then carbon backed, platinum shadowed, and then dissolved to allow viewing of the shadowed carbon in an electron microscope. The upper view shows the usual case where the abundant cosmic ray tracks (Crozaz et al., Fleischer et al., 1970) are etched and replicated to reveal tracks of several microns length. The lower view shows crystal 12028, 111, 30.3, 2, etched in the same manner but with much shorter tracks being revealed. Slip lines cover the field of view and are correlated with the track lengths: where the slip spacing is relatively wide ($\approx 0.7\mu$), the tracks are typically $\sim 0.7\mu$ long; where the slip spacing is reduced to $\sim 0.07\mu$, the track length is correspondingly less. In the light microscope (Leitz Ortholux at 1350X magnification) no tracks are visible in the region of fine slip, and recognizably short tracks are just discernible in the region of coarser slip. Superimposed on the approximately $3 \times 10^8/cm^2$ short tracks are $\sim 3 \times 10^5$ longer tracks that are uniformly distributed with no differences between the regions of fine and coarse slip. These longer tracks presumably correspond to irradiation of the sample by cosmic rays subsequent to the event which fragmented the original tracks. In short, the predeformation tracks are distinct from the post-deformation ones and should allow the sample history to be inferred.

If the tracks were known to be from spontaneous fission of uranium, as is normally the case for terrestrial samples, the chronological interpretation of the track densities would be straightforward because track production would be independent of the physical location of the sample. However, since the observed tracks are presumably from cosmic rays [the most abundantly observed tracks in lunar surface materials (Crozaz et al., Fleischer et al., 1970)], the number being formed at any time depends on the depth of burial (Fleischer et al., 1967). We therefore choose a specific model to illustrate the dating of deformation events--realizing, however, that the assumptions are merely plausible, not unique.

We assume then for simplicity that grain 12028, 111, 30.3, 2 (shown in Fig. 1, bottom) was located for a time T_1 at a constant depth of 600μ in the top of an exposed rock or in lunar soil. A time T_2 ago the crystal was deformed by the shock supplied by a meteoroid impact (the most commonly observed mode of deformation of lunar soil) and thrown to a new position near the surface as part of an ejecta layer. Since the grain was taken from a place near

*This work was supported by NASA under Contracts NAS 9-7898 and NAS 9-11583.

Manuscript received December 27, 1971.

Upper

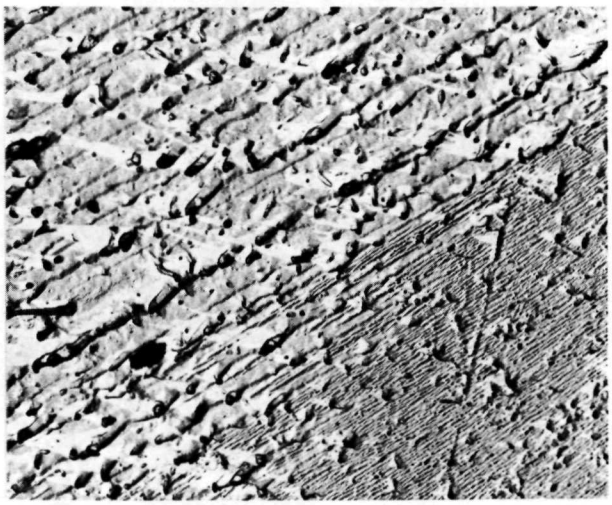

Lower

Fig. 1 Electron micrographs of replicas of tracks in lunar pyroxenes. The upper photo shows cosmic ray tracks in an undeformed pyroxene (sample 12028, 50, 11.5, 5); the lower photo shows sample 12028, 111, 30.3, 2, a 600μ diameter crystal with regions of fine slip (slip spacing <0.07μ) and coarser slip (slip spacing <0.7μ). The particle tracks are shortened to a length that is approximately the spacing of the slip lines. The height of each photo is approximately 26μ. Platinum-shadowed carbon replicas.

the bottom of layer III-2, which was about 4.4 cm thick when originally deposited on the surface (Comstock, 1971), we may assume that the grain was deposited at time T_2 at a depth of ~4 cm. It was then gradually covered by more and more soil until its depth in the soil reached about 43 cm, the depth at which it was removed from the moon as part of core sample 12028. By using the track accumulation rate (Comstock, 1971) appropriate to a depth of 600μ for the period T_1 and that for a gradual burial from 4 cm down to 40 cm, and using the observed track densities of short, deformed tracks, and long, undeformed tracks we derive the following history (if our assumptions on position are correct): This pyroxene crystal spent 20 to 25 m.y. at the lunar surface and then was shocked 20 to 25 m.y. ago and became part of an ejecta layer which spent $\lesssim$ 1 m.y. on the surface, prior to being covered ultimately by ~40 cm of soil from other impacts.

It should be evident that deformation dating constitutes a powerful tool for deciphering the history of lunar soil. For example, both the short burial time derived above and the existence of many pre-shock tracks support the concept of a complicated irradiation and redistribution history for the soil (Comstock, 1971; Comstock et al., 1971). The density of full-length tracks in grains that were severely shocked at their time of deposition should allow the deposition chronology to be calculated for a layered soil.

ACKNOWLEDGMENTS

We are pleased to thank E. Koch and M. McConnell for experimental assistance.

REFERENCES

Ahrens, T.J., R.L. Fleischer, P.B. Price, and R.T. Woods, Erasure of Fission Tracks in Glasses and Silicates by Shock Waves, Earth Planet. Sci. Let. 8, 420-426, 1970.

Berzina, I.G., I.V. Vorobeva, Ya. E. Gaguzin, and I.M. Zlotorv, Annealing of Tracks of Fragments from Spontaneous Fission of Uranium in Glasses and Mica Crystals, Solv. Phys. Doklady 11, 1105-1107, 1966.

Comstock, G.M., The Particle Track Record of the Lunar Surface, Proc. IAU Symposium #47, "The Moon", Newcastle, March 1971, G.E. Preprint 71-C-190.

Comstock, G.M., A.O. Evwaraye, R.L. Fleischer, and H.R. Hart, Jr., The Particle Track Record of Lunar Soil, Geochimica Cosmochimica Acta, Proc. 2nd Lunar Sci. Conf. 3, 2569-2582, 1971.

Crozaz, G., U. Haack, M. Hair, P. Hoyt, J. Kardos, M. Maurette, M. Miyajima, M. Seitz, S. Sun, R. Walker, M. Wittels, and D. Woolum, Radiation History of the Moon, Science 167, 563-566, 1970.

Fleischer, R.L., P.B. Price, and R.M. Walker, Effects of Temperature, Pressure, and Ionization on the Formation and Stability of Fission Tracks in Minerals and Glasses, J. Geophys. Res., 70, 1497-1502, 1965.

Fleischer, R. L., P. B. Price, R. M. Walker, and M. Maurette, Origins of Fossil Charged Particle Tracks in Meteorites, J. Geophys. Res. 72, 331-353, 1967.

Fleischer, R. L., P. B. Price, and R. M. Walker, Fission Track Dating and Processes in the Earth's Interior, in "Application of Modern Physics to the Earth and Planetary Interiors" S. K. Runcorn (Ed), Wiley-Interscience, N. Y., 1969, pp. 499-503.

Fleischer, R. L., E. L. Haines, R. E. Hanneman, H. R. Hart, Jr., J. S. Kasper, E. Lifshin, R. T. Woods, and P. B. Price, Particle Track, X-ray and Mass Spectrometry Studies of Lunar Material from the Sea of Tranquillity, Science 167, 568-571, 1970.

Fleischer, R. L., R. T. Woods, H. R. Hart, Jr., P. B. Price, and N. M. Short, Effect of Shock on Apatite and Sphene Crystals from the Hardhat and Sedan Underground Nuclear Explosions, to be published in 1972.

Fleischer, R. L., and H. R. Hart, Jr., Fission Track Dating: Techniques and Problems, Burg Wartenstein Conf. on Calibration of Hominoid Evolution July 1-12, 1971, W. Bishop, J. Miller, and S. Cole, Eds. Scottish Academic Press 1971, available as GE preprint 70-C-328.

Fleischer, R. L., and P. B. Price, Glass Dating by Fission Fragment Tracks, J. Geophys. Res., 69, 331-339, 1964a.

Fleischer, R. L., and P. B. Price, Techniques for Geological Dating of Minerals by Chemical Etching of Fission Fragment Tracks, Geochim. Cosmochim. Acta, 28, 1705-1714, 1964b.

Fleischer, R. L., and P. B. Price, Fission Track Evidence for the Simultaneous Origin of Tektites and Other Natural Glasses, Geochim. Cosmochim. Acta, 28, 755-760, 1964c.

Price, P. B., and R. M. Walker, Fossil Tracks of Charged Particles in Mica and the Age of Minerals, J. Geophys. Res., 68, 4847-4862, 1963.

Storzer, D., and G. A. Wagner, Correction of Thermally Lowered Fission Track Ages of Tektites, Earth Planet. Sci. Lett. 5, 463-468, 1969.

APPENDIX VIII

Earth and Planetary Science Letters (to be published)

GENERAL ELECTRIC

GENERAL ELECTRIC COMPANY
CORPORATE RESEARCH AND DEVELOPMENT
Schenectady, N.Y.

THE PARTICLE TRACK RECORD OF THE SEA OF PLENTY

by

G. M. Comstock, R. L. Fleischer, and H. R. Hart, Jr.,
General Physics Laboratory

Report No. 71-C-342 December 1971

TECHNICAL INFORMATION SERIES

CLASS 1

GENERAL ELECTRIC

General Electric Company
Corporate Research and Development
Schenectady, New York

TECHNICAL INFORMATION SERIES

AUTHOR Comstock, GM
Fleischer, RL
Hart, HR Jr.

SUBJECT lunar science

NO. 71-C-342

DATE December 1971

TITLE The Particle Track Record of the Sea of Plenty

GE CLASS 1

NO. PAGES 2

ORIGINATING COMPONENT
General Physics Laboratory

CORPORATE RESEARCH AND DEVELOPMENT SCHENECTADY, N.Y.

SUMMARY We have measured the particle track densities in 36 grains taken from two levels of the soil column returned from the Sea of Plenty by Luna 16. One sample is from near the surface; the other is from about 30 cm depth. All but two of the grains contained very high track densities, $>10^8/cm^2$. We conclude that all of the Luna 16 soil has been irradiated very close to the surface, that there has been little or no "recent" admixture of previously shielded material from below 30 cm, and that the regolith is both unusually thin at the Luna 16 site and extremely old (~3 b. y. or more).

KEY WORDS

lunar science, geology, particle tracks, cosmic rays

INFORMATION PREPARED FOR _____

Additional Hard Copies Available From

Corporate Research & Development Distribution
P.O. Box 43 Bldg. 5, Schenectady, N.Y., 12301

Microfiche Copies Available From

Technical Information Exchange
P.O. Box 43 Bldg. 5, Schenectady, N.Y., 12301

RD-54 (10/70)

THE PARTICLE TRACK RECORD OF THE SEA OF PLENTY*

G. M. Comstock, R. L. Fleischer, and H. R. Hart, Jr.

I. INTRODUCTION

Studies of lunar soil samples returned by the Apollo 11 and Apollo 12 missions have established that fossil nuclear particle tracks provide a useful record of the complex mixing and irradiation history of the soil.[1-3] The soil column returned from the Sea of Plenty by the automatic probe Luna 16 is a valuable sampling of an additional lunar site.[4] We have measured the energetic-particle track density in pyroxene, olivine, and feldspar crystals† from the first and fourth levels of the Luna 16 soil column. Our analysis is not yet complete, but the important results are clear.

II. OBSERVATIONS

Our soil allotment consisted of 5 mg from each of the depth intervals 0 to 8 cm [L-16-17A, designated "level 1," or Zone A[4]] and 28 to 32 cm (L-16-17G, "level 4," or Zone Γ). We etched all usable grains with diameter $\gtrsim 100\mu$. All but one of the several colorless, transparent grains behaved like low-efficiency glass rather than feldspar, i. e., etched features were shallow pits with a very low pit concentration of 2×10^4 to $3 \times 10^5/cm^2$. The usable non-glasslike samples are summarized in Table I. For the olivine crystals we used a new, more efficient etching solution reported by Lal;[5] for the others we followed our previous procedures.[6]

Only one of the samples in Table I could be accurately counted with the optical microscope. So far, only 11 have been replicated and counted using the transmission electron microscope; all of these were found to have track densities $\rho > 10^8/cm^2$ except for one ($\rho \sim 4 \times 10^7/cm^2$). Three of these had detectable track density gradients, in which cases the lowest density is the one quoted here. Also 29 etched crystalline samples have been assigned a preliminary lower limit based on optical counts; all of these have $\rho > 10^8/cm^2$. The distribution of track densities observed is shown in Fig. 1 and cumulative percentages are given in Table II.

TABLE I

Etched Crystalline Grains, Diameter $\gtrsim 100\mu$

	Level 1	Level 4	Total
Pyroxene	16	15	31
Feldspar	0	2	2
Olivine	9*	5*	8 etched
			41

*Six olivine crystals have not yet been sufficiently etched.

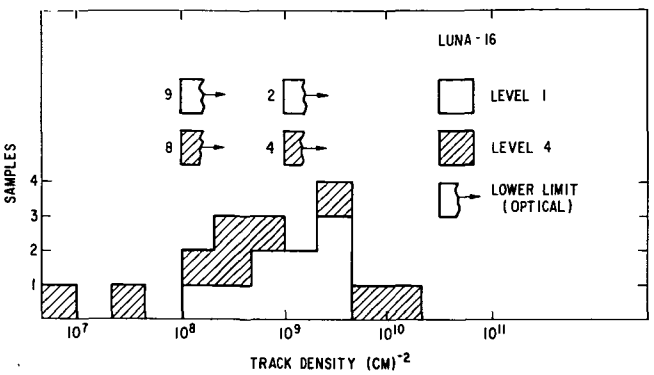

Fig. 1 Distribution of track densities from Level 1 (0 to 8 cm) and Level 4 (28 to 32 cm). All definite values were measured using a transmission electron microscope. In addition, the numbers to the left of the broken bars with arrows signify the numbers of crystals for which lower limits have been estimated optically.

TABLE II

Cumulative Track Density Distribution†

Density	Level 1	Level 4
$> 4 \times 10^7\ cm^{-2}$		95% (19)
$> 10^8\ cm^{-2}$	100% (21)	85% (17)
$\gtrsim 10^9\ cm^{-2}$	38% (8)	35% (7)

III. DISCUSSION

On the basis of our limited statistics, there is only a slight difference between layers 1 and 4. We find that both layers consist overwhelmingly of high-track-density grains. This is in sharp contrast with the Apollo 11 and Apollo 12 soils[1-3, 6] which contain many grains with $\rho < 10^8/cm^2$ in all layers.

Kashkarov[7] has measured the track densities in olivine crystals from five depth intervals in the Luna 16 soil column, and has found that the percentage of grains with $\rho > 5 \times 10^7/cm^2$ is close to 100% for the uppermost level 1 but decreases with greater

*This work was supported by NASA under Contract NAS-911583.

Manuscript received December 2, 1971

depth. It should be pointed out that Kashkarov used a less efficient etching solution for olivine, which may affect his results. However, he also found that 22 out of 25 grains (88%) with $\rho < 5 \times 10^7/cm^2$ contained track density gradients. This is much greater than the corresponding value of about 20% for Apollo 12 soil. (1, 2)

Very high track densities ($\rho > 10^8/cm^2$) and significant track density gradients within 100μ grains are both conclusive evidence for irradiation on or within a fraction of a millimeter of the lunar surface. (1) 100-micron-diameter grains will acquire our observed median density of 1 to 2 x $10^9/cm^2$ in $\sim 10^6$ years on the lunar surface but require $\sim 10^9$ years at a depth of 1 mm. Since there are 3000 100μ layers in 30 cm (the depth of level 4) the total time required for each of them to have spent $\sim 10^6$ years on the surface is $\sim 3 \times 10^9$ years, an approximate age of this maria surface.

IV. CONCLUSION

Essentially all of the Luna 16 grains have been irradiated within the top fraction of a millimeter of the lunar surface. Furthermore, for the soil sample studied, there has been little or no "recent" admixture of previously shielded material from much below 30 cm, which would have been detected by its low track densities. In fact, there is no time available in the "exposure budget" for material much below 30 cm at the Luna 16 site to have been irradiated near the surface as completely as the soil sample studied.

These properties imply that the soil has not been mixed or "gardened" much deeper than 30 cm, which means that the regolith is relatively shallow at the Luna 16 site. This is consistent with the observation that the sampled soil column becomes coarser near the bottom. (4)

ACKNOWLEDGMENTS

We are pleased to give thanks to W. R. Giard, M. D. McConnell, and G. E. Nichols for experimental assistance.

REFERENCES

1. G. M. Comstock, "The Particle Track Record of the Lunar Surface," Proc. I. A. U. Symposium No. 47, "The Moon," Newcastle upon Tyne, England (1971), in press.

2. G. M. Comstock, A. O. Evwaraye, R. L. Fleischer, and H. R. Hart, Jr., "The Particle Track Record of Lunar Soil," Proc. Second Lunar Science Conf., 3, MIT Press (1971), p. 2569.

3. G. Arrhenius, S. Liang, D. MacDougall, L. Wilkening, N. Bhandari, S. Bhat, D. Lal, G. Rajagopalan, A. S. Tamhane, and V. S. Venkatavaradan, "The Exposure History of the Apollo 12 Regolith", Proc. Second Lunar Science Conf., 3, MIT Press (1971), p. 2583.

4. A. P. Vinogradov, "Preliminary Data on Lunar Ground Brought to Earth by Automatic Probe 'Luna 16'," Proc. Second Lunar Science Conf., 1, MIT Press (1971), p. 1.

5. S. Krishnaswami, D. Lal, N. Prabhu, and A. S. Tamhane, "Olivines: Revelation of Tracks of Charged Particles," Science 174, 287 (1971).

6. R. L. Fleischer, E. L. Haines, H. R. Hart, Jr., R. T. Woods, and G. M. Comstock, "The Particle Track Record of the Sea of Tranquillity," Proc. Apollo 11 Lunar Science Conf., 3, MIT Press (1971), p. 2103.

7. L. L. Kashkarov, personal communication.

† Note added in proof. Examination of ten glass samples revealed tracks only in one pair of co-existing samples (160,000/cm^2 and 22,000/cm^2). In four cases track densities could be observed in crystals surrounded by the glass, the ratios of track densities (in crystal/in glass) being >230, >500, >800, and >8000 with 95% confidence. Since differences in etching efficiency can account for at most a ratio of 10, we conclude that track fading in the glass makes those results not pertinent to this discussion.